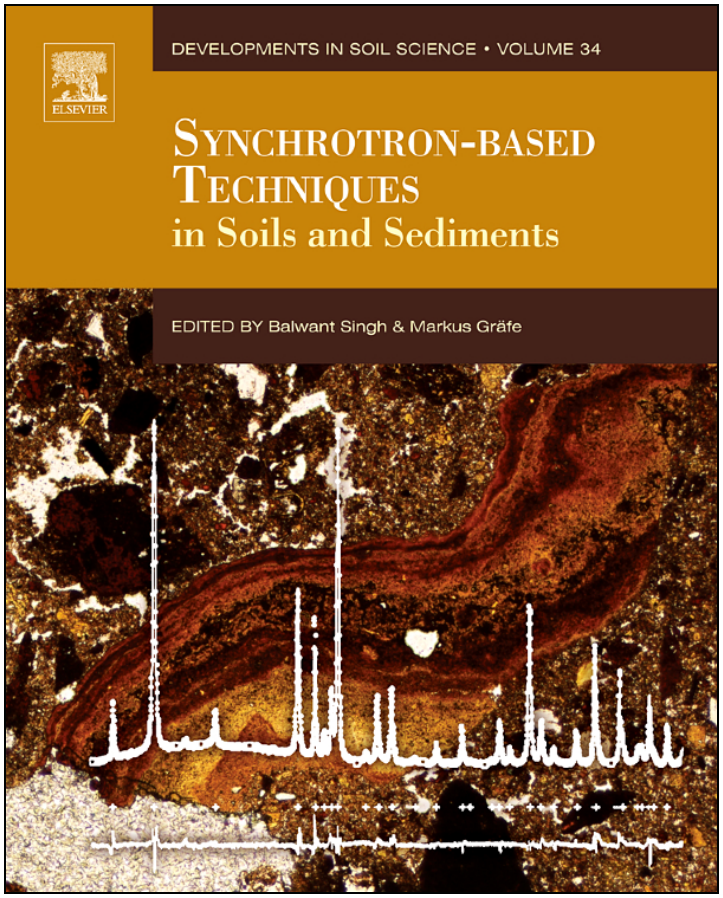

From: Hoi-Ying N. Holman, Synchrotron Infrared Spectromicroscopy for Studying Chemistry of Microbial Activity in Geologic Materials. In Balwant Singh and Markus Gräfe: Developments in Soil Science, Vol. 34. Elsevier B.V., The Netherlands, 2010, pp. 103-130.
ISBN: 978-0-44-453261-9

CHAPTER

4

Synchrotron Infrared Spectromicroscopy for Studying Chemistry of Microbial Activity in Geologic Materials

Hoi-Ying N. Holman

Ecology Department, Earth Sciences Division, and Virtual Institute for Microbial Stress and Survival, Lawrence Berkeley National Laboratory, University of California, Berkeley, California, USA

OUTLINE

1. INTRODUCTION

Recent large-scale gene sequencing (Baker et al., 2003), functional metagenomic (Dinsdale et al., 2008; Mou et al., 2008), and metaproteomic profiling (Ahmed-Omer et al., 2007) of many microbial niches on our planet is beginning to transform many research areas in environmental and earth sciences. These analyses yield the "blueprints" for microbial genetic, regulatory and metabolic processes that can affect geological materials (Kashefi et al., 2002;

Macalady and Banfield, 2003; Salmassi et al., 2002). They also form an emergent base which allows research to focus on understanding how microbial systems and their metabolic processes shape the biogeochemistry and quality of terrestrial environments. A biogeochemical system approach will facilitate a broad range of innovative biotechnology applications to soil science, such as enhancing nutrient cycling and productivity or detoxification of recalcitrant environmental pollutants. Synchrotron radiation-based Fourier transform infrared (SR-FTIR) spectromicroscopy can be used to monitor noninvasively some of the chemical changes induced by microbial activity. In this chapter, we review how SR-FTIR spectromicroscopy can potentially make an important contribution to earth sciences through noninvasive high-resolution experimental measurements of microbial activity on surface of geologic materials.

1.1. Defining Synchrotron Radiation-Based Infrared Spectromicroscopy

SR-FTIR spectromicroscopy is a high-resolution analytical technique that allows one to probe chemical and cellular processes with a temporal resolution in the range of seconds to minutes and a micrometer-scale spatial resolution. SR-FTIR spectromicroscopy combines the advantages of three existing technologies: (1) conventional midinfrared spectroscopy, which exploits the fact that vibrational spectra are molecular/material characteristics; (2) using microscopy to visually locate interesting targets and focus infrared light on them for molecular/material analysis; and (3) the high signal-to-noise ratio furnished by the extremely bright synchrotron radiation-based infrared light source. A synchrotron light source is a high-energy electron storage ring optimized for production and collection of the intense light radiated by electrons accelerated to nearly the speed of light, as illustrated in Fig. 4.1. Because the opening angle of radiation emitted from relativistic electrons in a synchrotron storage ring is very small, the effective source size of infrared radiation source is dominated by diffraction, due to the nature by which waves propagate; and thus can be considered as a nearly ideal point source (Sham and Rivers, 2002).

Conventional infrared spectroscopy uses radiation from a thermal emission element or a thermal globar as its infrared light source. Using infrared spectroscopy with microscopy has traditionally been associated with viewing a sample that can be as small as a millimeter or less, and determining the chemical composition of that small sample as measured by the infrared spectra "as it is," In this sense, infrared spectromicroscopy of biological and geological materials already dates back to the late 1940s when researchers began to demonstrate the potential of joining infrared spectroscopy with microscopy (Barer et al., 1949; Blout et al., 1949; Gore, 1949), and built infrared spectral databases using then newly developed infrared spectroscopy techniques (Barer, 1949, 1953, 1954; Barer and Joseph, 1954; Bird and Blout, 1952; Blout, 1953). As the quality of detectors and spectrometers improved, their work yielded extensive spectral databases of many biological and geologic materials. However, making spectral measurements on microscopic features was difficult because the infrared spectrometer was not directly coupled to the microscope. In the 1990s, the rapid development in microprocessor and computational technologies removed these difficulties and enabled FTIR spectromicroscopy (also called microspectroscopy) to emerge as a powerful analytical tool (Wetzel and LeVine, 1999). The then new FTIR spectromicroscopy technique (Fig. 4.2) directly coupled the infrared spectrometer to a microscope, all to identify and target microscopic structures in a sample, use

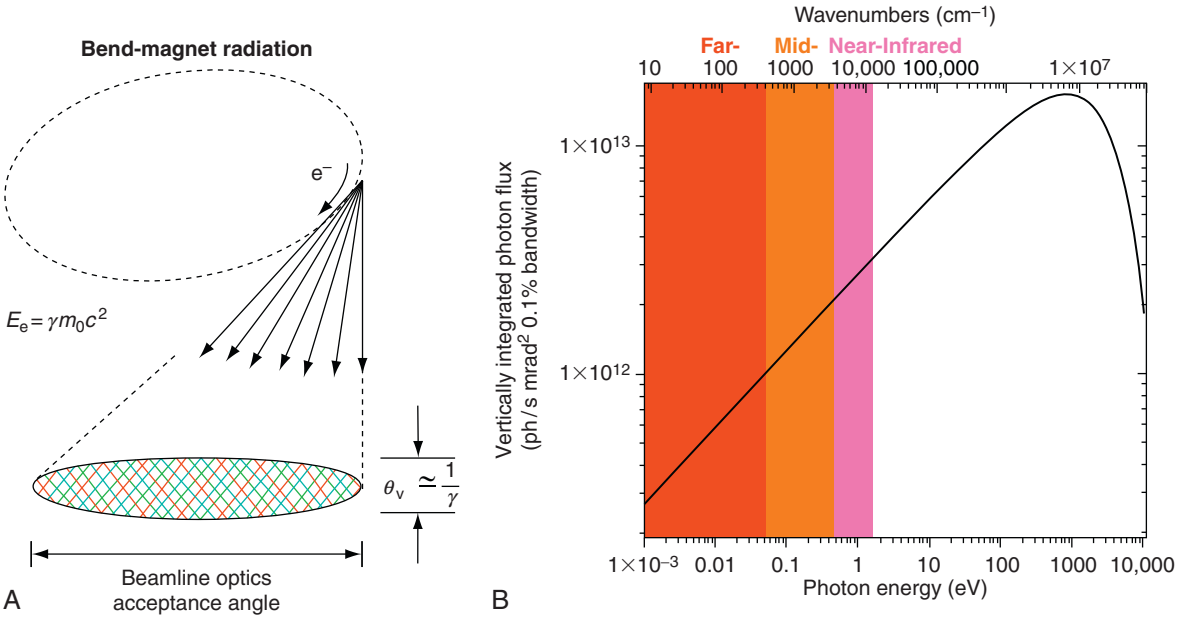

FIGURE 4.1 An overview of synchrotron radiation. (A) Guided by a series of bending magnets and straight sections, relativistic electrons inside a storage ring complete a loop. When the relativistic electrons encounter a magnetic field, they are deflected and they emit electromagnetic radiation with energy photons up to hard X-rays. (B) This so-called bending magnet spectrum extends from very low energies (far-infrared) continuously to a critical energy in the soft or hard X-ray, depending on the energy of the synchrotron. The radiation pattern from relativistic electrons is such that its effective source size can be considered as very close to an ideal point source.

an aperture to target the area of interest within the sample, and collect transmitted or reflected infrared radiation from that targeted area onto a detector. In general, thermal emission sources can be focused with an infrared microscope to a spot of 75-100 μm in diameter. To measure smaller features, one needs to use an aperture to mask away part of the incoming infrared light, or distribute the incoming light among an array of detectors, which can significantly reduce the signal strength.

Unlike the conventional source, a synchrotron infrared source enables one to obtain spectra from targeted areas whose size approaches the diffraction limit without using an aperture (Carr, 1999). Thus for SR-FTIR spectromicroscopy, the infrared beam can be focused visibly to a spot with a diameter of its wavelength, which yields a spatial resolution 0.7 times wavelength (Levenson et al., 2006, 2008a,b). For mid-IR wavelengths of 2.5-25 μm, SR-FTIR spectromicroscopy enables one to obtain spectra on targeted areas of ~2-20 μm in diameters. Comparative experimental measurements have shown a two to three orders of magnitude signal-to-noise advantage for synchrotron-based measurements (Holman et al., 2003). The high signal-to-noise ratio also allows one to acquire good quality spectra on a microscopic area by averaging the signal over several seconds to minutes instead of hours (Panero et al., 2003; Fig. 4.3). Panero et al. (2003) mounted a tiny piece of ocean basalt in a diamond anvil cell to achieve extremely high pressures and

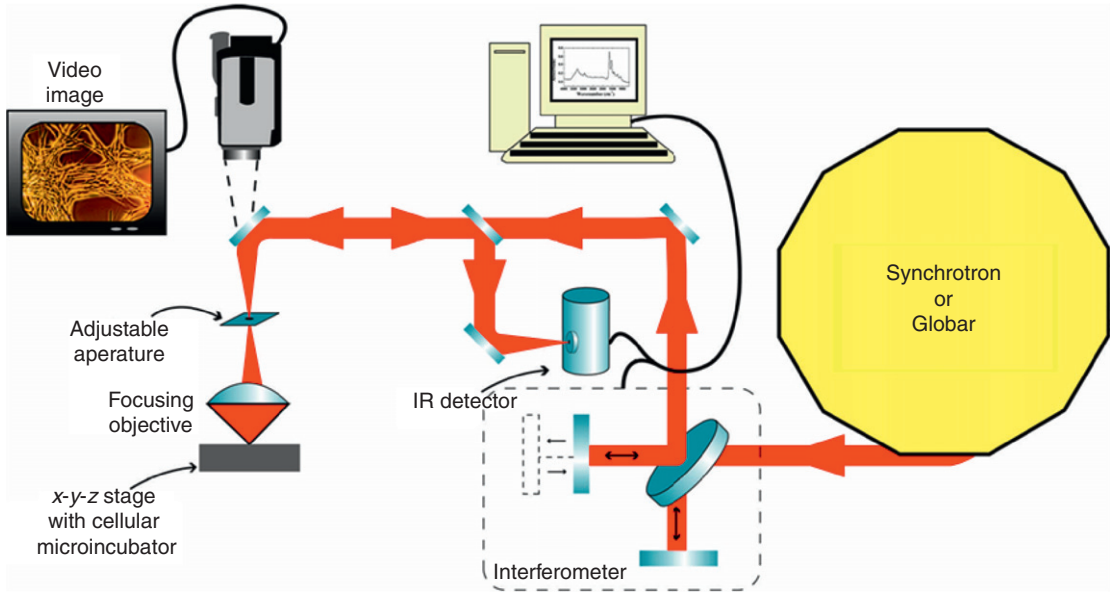

FIGURE 4.2 Schematic diagram of Fourier transform infrared (FTIR) spectromicroscopy experimental setup. Mid-infrared radiation from either a synchrotron or a globar is transported to a FTIR interferometer bench. After modulation by the interferometer, an infrared microscope focuses the beam onto the sample with all-reflecting optics. Microbial or biogeochemical samples can be placed inside an on-stage mini-incubator with environmental controls. The stage is computer controlled and rasters the sample in the *x-y-z* plane to ± 0.1 m precision to obtain spectral maps across the sample. The light reflected from the sample is collected by the same microscope optics and sent to an IR detector. A computer performs a Fourier transform on the measured interferogram to obtain an infrared spectrum.

measured infrared absorbance of the sample at a pressure of 32 GPa. When using a conventional FTIR spectromicroscopy system, averaging the signal over seven hours and 60,000 scans was required to detect the spectral features. Using a synchrotron light source, a significantly improved spectrum was obtained after averaging 256 individual scans recorded over a 2 min period.

1.2. Why Is SR-FTIR Spectromicroscopy Necessary?

Essential to understanding the roles of microbial activity in soil or sediment environments is the ability to measure how microorganisms interact with those environments through their wide range of metabolic capabilities. Many studies have found that microbial interactions with sediments occur primarily at the microbe-substrate interface itself and that the interfacial properties are quite variable. At a microscopic scale of 1-100 μm that variation is due to (1) clusters of microorganisms that differ in their metabolic activity and to (2) spatial variations in reactive molecules of metal oxides and organic molecules. At present the laboratory methodology commonly employed to study these heterogeneous biogeochemical phenomena is a combination of microscopic imaging and conventional or synchrotron radiation-based X-ray spectroscopy techniques (see other book chapters). X-ray spectromicroscopy studies of natural or model materials have

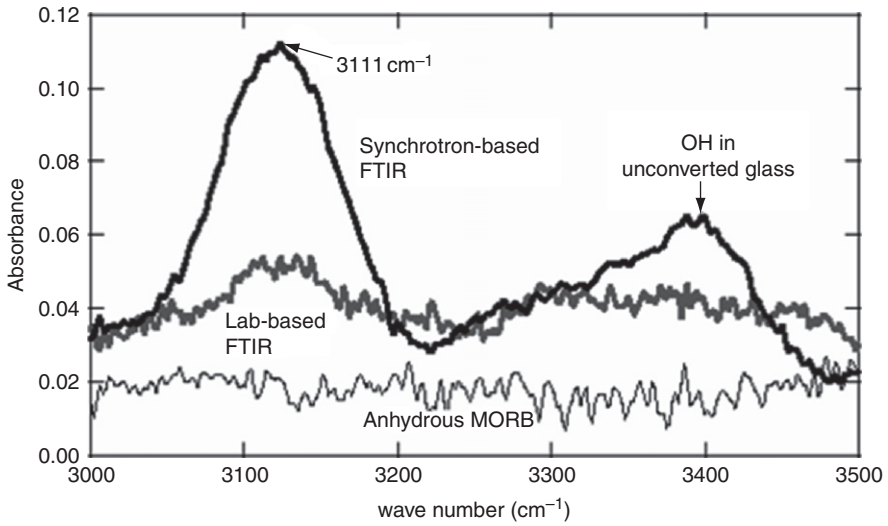

FIGURE 4.3 Spectra of a sample synthesized at 32 (±2) GPa and 2850 (±150) K, comparing results from a synchrotron-based system (black, Advanced Light Source beamline 1.4.3; Nicolet Magna 760 with KBr beamsplitter and an MCT detector) to the spectrum from a lab-based system (gray, Bruker IFS-66v using a CaF2 beamsplitter and an InSb detector). The collection time for the synchrotron-based system was about 2 min (256 scans, top), compared to about 7 h (60,000 scans, bottom) for the lab-based system. While both show a distinct peak at 3111 cm^{-1} corresponding to OH vibrations in stishovite, the synchrotron-based spectrum has a better signal-to-noise ratio, as well as better spatial resolution. There is no detectable absorption at 3450 cm^{-1}, where OH in Mg-perovskite is expected to absorb. A control experiment was performed on a dry, synthetic basalt glass starting material (sample 1114b_6); synthesis conditions were 33 (±1) GPa and 2130 (±150) K. No absorption features were found in the 3000-3500 cm^{-1} region for this sample (thin line, bottom), again collected by synchrotron FTIR (Panero et al., 2003).

provided important and unique information about how microorganisms interact with sediments. However, X-ray spectromicroscopy techniques entail energies of tens to thousands of electron volts (eV), which adversely affect or even kill microorganisms and thereby limit X-ray spectromicroscopy to measuring biogeochemical processes at single (rather than continuous) time points. Therefore, new methods are needed to study ongoing processes in living microbes at a scale of spatial heterogeneity that is relevant for microbial actions in sediments.

SR-FTIR spectromicroscopy is well suited to meet that need. The bright infrared light emitted from a synchrotron source permits rapid and high quality measurements for the spectral characterization of microscopic geologic materials (Hofmeister, 1995) while inducing little or no detectable effect on bacteria (Holman et al., 2009a). The nonintrusive and high-resolution SR infrared beam allows one to use SR-FTIR spectromicroscopy to make time-sequence spectral measurements uninterruptedly while biological and chemical processes continue. Currently, the temporal resolution for geologic material measurements is shorter than one minute. SR-FTIR spectromicroscopy has been used to make real-time sequential measurements of the reduction of hexavant chromium (Cr(VI)) by living basalt-inhabiting bacteria from a heavy metal polluted site

(Holman et al., 1999) as well as the destruction of pyrene by colonies of soil bacteria inhabiting a Superfund site (Holman et al., 2002). More recently, SR-FTIR spectromicroscopy was used to study the intracellular chemistry of obligate anaerobic bacteria to understand how they survive in transiently oxygenated soils and sediments (Holman et al., 2009b).

Another advantage of SR-FTIR spectromicroscopy is that once the beam is focused on the sample, spatially resolved mapping can be accomplished by moving the sample under the beam. In this manner, the microscopic heterogeneity of a macroscopic sample can be examined or even profiled at diffraction-limited spatial scales. For example, SR-FTIR spectromicroscopy has been used to analyze hydrocarbons in minerals (Bantignies et al., 1995; Guilhaumou et al., 1998; Lu et al., 1999) and in sediments (Ghosh et al., 2001). The technique has also been used to reveal the spatial coincidence of microbial activity and pollutant transformation (Holman et al., 1999, 2002, 2009a), to characterize metal-cyanobacteria sorption reactions in aqueous environments (Yee et al., 2004b) and the effect of land use on the composition of soil organic matters (Solomon et al., 2005).

2. EXPERIMENTAL PROCEDURES

The nature of an SR-FTIR experiment governs its procedures. To illustrate, consider an experimental analogue of microbial activity in contaminated sediments. Our goal is to identify and characterize microbial abilities to detoxify surrounding pollutants. There are essentially two types of experimental systems: intrinsic microbe/geologic material systems and model microbe/geologic material specimen systems. Materials used in an intrinsic experimental system are taken directly from polluted sites; whereas materials used in a model experimental system are generally known microbial isolates and geologic materials whose complexities range from crystals of a single mineral to composite geologic materials. Spectra are usually obtained in reflection collection modes, but can also be obtained in a transmission collection mode; the choice depends on experimental design and the optical properties of the geologic materials and the thickness of the specimens.

2.1. Sample Examination and Preparation

The quality of the geologic material substrates or specimens is one of the single most important factors for successful applications of SR-FTIR spectromicroscopy to soil and sediment research. A visual examination of a geologic material sample under the stereoscope (which should be housed in a sterile hood if contamination is to be avoided) is the first step. This viewing allows one to appraise the overall surface topography and surface quality of the sample so that one can start the SR-FTIR spectromicroscopy experiments with a promisingly smooth geologic material sample.

Then improve the quality of the "promising" sample to minimize potential unwanted effects that would diminish the quality of infrared spectra; address scattering, for example, by removing uneven microscopic grains or particles that protrude from the surface using fine-pointed probes and micro-forceps. Use microliter pipettes to apply small amounts of "sterile" liquid to keep the sample's microbes alive during examination.

Additional steps are needed for a model microbe/mineral specimen system. First, cleave protruding fragments from the specimen by using, for example, a mini-hammer or small chisels. Some helpful information can be found in literature (Hofmeister, 1995; Teetsov, 1995). Then clean the specimen surfaces by sonification in deionized and organic-free water, and

sterilize the surface with UV-irradiation. Place the specimen inside a sterile microscope chamber (see Section 2.3) and use the microscope component of the SR-FTIR spectromicroscope to identify surface area to be studied. The selection of the area is relatively subjective and relies on the geometry, color, crystallographic properties, and other material-specific features of the sample surface. Record the infrared spectra from selected surface area. After making these SR-FTIR measurements of the surface, apply a microscopic volume of environmental material collected from field sites and microorganism suspension, sequentially or in a mixture, onto the surface using sub-microliter syringes. SR-FTIR measurements are preferably made following each material/suspension application.

2.2. SR-FTIR Instrumentation

The SR-FTIR spectral measurement of microbial activity on geologic materials requires coupling a commercially available FTIR spectromicroscopy system to a synchrotron light source (Fig. 4.2). At some synchrotron infrared facilities, the SR infrared beam is also passed through a beam position locking system (McKinney et al., 2000; Scarvie et al., 2004) (Fig. 4.4) to restrain beam movements to less than 1 m. Without this system, the beam tends to move about the sample by several micrometers during data acquisition, producing artifacts and/or noise in the data. The beam-locking system is exceedingly helpful when studying biogeochemical materials that often have fine and highly heterogeneous surface features.

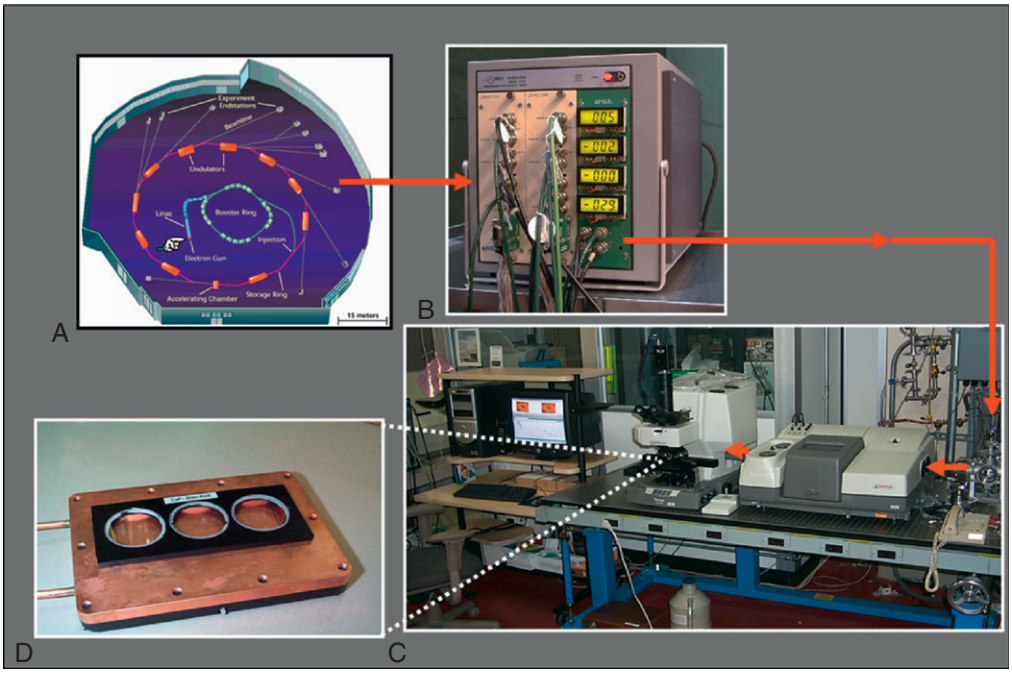

FIGURE 4.4 The beam position locking system instrumentation at Beamline 1.4.3 at the ALS. It is specifically made for probing biogeochemical processes *in situ* and *in vivo*. The beam from the synchrotron (A) is passed through the beam position locking system (B), then enters the commercially available FTIR spectromicroscopy system (C). During the experiment, samples are kept inside a stage mini-incubator (D). The addition of the beam-locking system is exceedingly helpful when studying biogeochemical materials that often have fine and highly heterogeneous surface features.

For real-time sequential SR-FTIR measurements, samples are maintained inside a mini environmental chamber (Fig. 4.4) that is mounted on the microscope stage. The sample is positioned using a computer-controlled *x*-*y*-*z* stage with 0.1-μm precision, allowing mapping measurements of FTIR spectra (through the incubator's ZnSe window) as a function of *x*- and *y*-position on the sample. Once the area to be studied has been identified, focus the point-like synchrotron infrared beam onto the target area; SR-FTIR spectra can then be recorded.

2.3. Microscope Stage Environmental Chamber

To reliably study microbially induced chemical changes in sediments, SR-FTIR spectromicroscopy measurements should be made in well-controlled experiments that simulate microbial viability and functionality under *in situ* conditions. This is important because microorganisms are exceedingly sensitive to their immediate environments and the microbes themselves alter associated sediments and environmental materials, mostly as a consequence of metabolic activity (Ehrlich, 1994, 1998, 2000; Macalady and Banfield, 2003; Newman and Banfield, 2002; Reysenbach and Shock, 2002). Important environmental conditions include temperature, pH, redox potential (Eh), available nutrients, chemistry of the pore water, relative humidity, and gas composition. For example, temperature can significantly affect the rate of microbial transformation of redox-sensitive elements such as iron and sulfur. Increasing temperature can increase microbial metabolism and oxygen consumption (Hines et al., 1982), decreasing the redox potential (Lyons et al., 1979; Sorensen et al., 1979). Changing the redox potential can shift the relative importance of specific terminal electron acceptors used in bacterial respiration (Revsbech et al., 1980; Sorensen et al., 1979). A decrease in redox potential can also affect the chemical and physiochemical state of redox-sensitive elements and thereby alter the chemistry of the bacteria themselves as well as of the overlying thin film of water (through changes in diffusional fluxes and other processes). To reliably study molecular changes in this chain of biogeochemical events, SR-FTIR spectromicroscopy measurements must be made in experiments that simulate *in situ* conditions using well-controlled flow through cells with infrared-transparent windows. Currently, several research groups are developing various types of automated microfluidic incubation platforms that allow one to rapidly manipulate these experimental conditions. Some of these platforms also control the thickness of the water film to permit infrared monitoring of the microbial processes in aqueous environments (Holman et al., 2009a). Nano-scale sensors are also being developed to provide additional measurements of physiological and geochemical parameters occurring below a micrometer spatial resolution.

3. ISSUES ASSOCIATED WITH SPECTRA ANALYSIS AND INTERPRETATION

Because of the complexity of a biogeochemical system, the spectrum contains the total absorption of many ingredients present in the path within the diffraction-limited area. A key effort has been to carefully identify infrared reflection-absorption or transmission-absorption spectral features that are truly molecular markers of the biogeochemical phenomena to be investigated. As highlighted in Table 4.1, infrared spectra of biomolecules in microbes and many relevant minerals are already well known; and likewise (Table 4.2) for common environmental pollutants. Hence, specific peaks and groups of peaks can be related to specific biochemical and chemical groups of

TABLE 4.1 A summary of example references for minerals and biomolecules

Substances	References
Rock-forming minerals	Keller et al. (1952)
Monolayers-normal-hexanethiol on Zn minerals	Eyring and Wadsworth (1956)
Soil	White (1971)
Minerals	Farmer (1974)
Minerals	Povarennykh (1978)
Asbestos minerals	Luys et al. (1982)
Granite, calcite, talk	Arnold and Wagner (1988)
Alunitic, kaolinitic, illitic, and propylitic type minerals	Collins (1991)
Extracellular polysaccharides	Ha et al. (1991)
Soil	Nguyen et al. (1991)
Garnet	Rossman and Aines (1991)
Hydrous alkali uranyl silicates and hydrous uranyl silicate minerals	Plesko et al. (1992)
Garnet, omphacite and kyanite	Beran et al. (1993)
Kaolinitic soil clays	Kretzschmar et al. (1993)
Oleate molecules on apatite	Mielczarski et al. (1993)
Kaolinite	Delineau et al. (1994)
Asteroid minerals	Vilas et al. (1994)

single molecules in an ideal system. The traditional approach of spectral analysis, which is intended to identify particular compounds, involves a band-shape analysis followed by direct assignment of characteristic absorption bands in the infrared spectrum. However, in a complicated and often transient biogeochemical system under *in situ* and *in vivo* conditions, these specific peaks and bands of peaks may shift, and the overall pattern may even change and deviate from their characteristic features. The spectral character can be complicated further by the surface and matrix properties of sediments. Interference fringes can obscure interesting spectral information while distorting and exaggerating less informative bands. Moreover, silicates and other highly polarizable materials may yield misleading spectral features.

One general approach is to focus on a small number of characteristic spectral features that were observed in a series of simplified model systems performed prior to the SR-FTIR spectromicroscopy experiment. For time-course experiments, this approach combines the traditional approach of direct band assignments and difference spectroscopy to guide the interpretation of the absorption bands as a function of time. It evaluates the intensity of each absorption band by means of the method of the most probable baseline (Lijour et al., 1994). It is important to note that as the beam current of the synchrotron decreases with time between electron refills, the beam intensity decreases proportionally; this must be taken into account if one wants to accurately measure absorption band intensity. We have found that rescaling the intensity of the absorption bands by means of an internal-standard-equivalent approach works reliably.

Prior knowledge of the type of the pollutants and the pathways of their possible biogeochemical transformation is nearly prerequisite to successful application of SR-FTIR spectromicroscopy. For example, heavy metal and metalloid pollutants comprise a most difficult environmental problem because they cannot be destroyed once released into the environment. A key goal of using SR-FTIR infrared spectromicroscopy is to characterize how intrinsic microorganisms affect the speciation of these heavy metals and metalloids, for speciation dictates their overall mobility, bioavailability, toxicity and other health risks in the biosphere. Hence, we need fundamental knowledge as the stability and mobility of the parent metal compounds, their interactions with microorganisms, and the altered stability and mobility

TABLE 4.2 A summary of example references for common environmental pollutants

Substances	References
Chromium and molybdenum hexacarbonyls	Hawkins et al. (1955)
Pentacyanonitrosyl-complexes of chromium and molybdenum	Griffith et al. (1959)
Aromatic chromium tricarbonyls	Humphrey (1961)
Explosive molecule vapors(TNT, RDX, and PETN)	Janni et al. (1997)
polycyclic aromatic hydrocarbons(PAHs):nitrogen/oxygen substitution	Bauschlicher (1998)
PAHs: methyl substitution and loss of H	Bauschlicher and Langhoff (1998)
PAHs containing two to four rings	Hudgins and Sandford (1998a)
PAHs containing five to more rings	Hudgins and Sandford (1998b)
Fluoranthene and benzofluoranthenes	Hudgins and Sandford (1998c)
PAHs incorporating a cyclopentadienyl ring	Hudgins et al. (2000)
Organo-arsenic(III), -antimony(III) and -bismuth(III) thiolates	Ludwig et al. (2000)
PAHs	Pauzat and Ellinger (2001)
PAHs incorporating the peropyrene structure	Mattioda et al. (2002)
Nonregular PAHs	Pauzat and Ellinger (2002)
large PHAs	Ruiterkamp et al. (2002)
Explosive and explosive vapors(TNT, TATP, RDX, PETN and Tetryl)	Todd et al. (2002), Seelenbinder and Brown (2002)
Naphthalene and anthracene	Abdullah et al. (2003)
1-nitropyrene	Carrasco-Flores et al. (2004)
Toluene-3,4-dithiolatoantimony(III) derivatives	Chauhan et al. (2004)
Trimethylarsine oxide	Jensen and Jensen (2004)
phosphorus tricyanide	Jensen (2004)
Oil spill	Li et al. (2004)
Quinoline and Phenanthridine in Solid Argon and H_2O	Bernstein et al. (2005)
6-nitrochrysene	Carrasco-Flores et al. (2005)
Arsenate on Fe-Ce bimetal oxide	Zhang et al. (2005)

of intermediate products under *in situ* and *in vivo* conditions. Our approach to this issue has been both fundamental and applied in nature. We often complement the SR-FTIR spectromicroscopy experiments with successive *in vitro* and *in vivo* studies of model systems of varying complexity in order to approximate membrane permeability, biotransformation, and toxicity. This enabled us to identify key functional group targets, which needs to be measured and to ensure that these targets are likely to be in the biogeochemical system to be investigated.

As an illustration, consider a SR-FTIR measurement of microbial transformation and detoxification of chromium in geologic materials. Chromium is a redox-sensitive metal pollutant that enters the environment primarily from industries such as leather tanning, wood preservation, metal plating and alloying (Nriagu, 1988). The two important oxidation states of chromium commonly found in natural

environments are trivalent [Cr(III)] and hexavalent [Cr(VI)] states, which have widely contrasting mobility and bioavailability (Bartlett and James, 1988). Most Cr(VI) compounds are highly soluble in water and are readily bioavailable to ecological receptors, while most Cr(III) compounds are distinctly less water soluble and less bioavailable. Cr(VI) compounds are amongst the earliest chemicals to be classified as mutagens and human carcinogens (International Agency for Research on Cancer, 1990; Levina et al., 2003; Stern, 1982). Its genotoxic and carcinogenic effects derive from its ability to enter cells rapidly through nonspecific transport mechanisms. Once inside, intracellular biomolecules such as polysaccharides, L-ascorbic acid, glutathione and other reductases readily reduce Cr(VI) species to formed an array of genotoxic Cr(III) complexes and other radicals that can cause single-strand-breaks and plasmid DNA nicking as well as a wide variety of DNA lesions and additional oxidative damage (Codd and Lay, 2001; Dillon et al., 1997; Levina et al., 1999; Snow, 1991; Sreedhara et al., 1997; Tsou et al., 1997; Voitkun et al., 1998). But in the environment, Cr(III) is considered insoluble and/or nongenotoxic. Biogeochemical processes that reduce Cr(VI) to Cr(III) compounds in the environment are therefore very significant for reducing chromium toxicity. Many indigenous bacteria in chromium-polluted environments possess several survival mechanisms that can potentially transform soluble chromium to less soluble forms. Our experiments show that some Cr-resistant microorganisms immobilize and reduce Cr(VI) to stable Cr(III)-complexes extracellularly through interactions with diverse groups of biomolecules (Codd and Lay, 1999, 2001; Codd et al., 1997; Gez et al., 2005; Levina et al., 2004) and the formation of genotoxic intermediates Cr(V)- and Cr(IV)-complexes (Kalabegishvili et al., 2003; Tsibakhashvili et al., 2002a). Concern exists that Cr(III) (as $Cr(OH)_3$) can be reoxidized to form Cr(VI) compounds (Chinthamreddy and Reddy, 1999). Our preliminary SR-FTIR spectromicroscopy results indicate that only a small fraction of Cr(III) compounds exist as $Cr(OH)_3$ in microbial systems.

Another illustration is microbial destruction of organic pollutants. Unlike heavy metals, organic pollutants can be destroyed. Once they have entered into the biosphere, they can be degraded, metabolized, and/or mineralized by many intrinsic bacteria by the many possible pathways that differ in complexity and kinetics (Bryant et al., 1991; da Silva et al., 2003; Furukawa, 2000, 2003; Furukawa et al., 1993, 2004; Hale et al., 1990, 1991; Kim et al., 2004; Kumamaru et al., 1998; Misawa et al., 2002; Pothuluri et al., 1995, 1998a,b, 1999; Suenaga et al., 2001, 2002). Much pathway information is available at the University of Minnesota Biocatalysis/Biodegradation Database (http://umbbd.ahc.umn.edu/). However, many pathways and the toxicities of intermediates are still unknown. Further, how environmental factors affect microbial abilities to degrade organic pollutants remains poorly known. Our current approach using SR-FTIR spectromicroscopy to study biodegradation of organic pollutants by intrinsic microorganisms is more applied than fundamental. We seek to address whether those microorganisms already in place can decompose the organic pollutants present and what geochemical factors are responsible for the bioavailability of the organic pollutants to microorganisms. For microorganisms that degrade organic pollutants by a known pathway, we intend to address whether intermediates are persistent and/or harmful to ecological receptors (Holman et al., 2002).

Finally, it is important to realize that information derived from SR-FTIR spectromicroscopy is but the tip of an iceberg. Because of the complexity of a biogeochemical system, this information alone is not sufficient for a thorough understanding of how intrinsic microorganisms transform pollutants and what factors

could alter the microbe's ability to transform the pollutants. It is also not sufficient for making reliable predictions of the potential risks of these pollutants and intermediates pose to ecological receptors and humans. The use of multiple complementary biochemical, analytical, and imaging techniques is thus necessary. An example of the use of complementary techniques is the collaborative study by researchers from the Lawrence Berkeley National Laboratory (USA) and the Georgian Academy of Science (Republic of Georgia) of chromium reduction by basalt-inhabiting aerobes (Abuladze et al., 2002; Asatiani et al., 2004; Kalabegishvili et al., 2003; Tsibakhashvili et al., 2002a,b, 2004). In addition to using SR-FTIR spectromicroscopy to track the sequential reduction of chromium, they are also using sodium dodecylsulfate polyacrylamide gel electrophoresis (SDS-PAGE) to identify chromium-induced changes in cell-wall protein composition (Abuladze et al., 2002), capillary electrophoresis to determine the effect of cell-wall proteins on the mobility of chromium through the cell wall (Tsibakhashvili et al., 2002a), electron spin resonance (ESR) to determine/confirm chromium speciation in bulk cells (Kalabegishvili et al., 2003), and μXRF and μXAFS imaging of Cr, Fe and Mn distributions on surface of basaltic rock specimens. Synergistic use of an array of different analytical techniques allowed these researchers to discover the unexpected accumulation and immobilization of stable and toxic chromium intermediates by microorganisms, which has significant implications for using intrinsic microorganisms to remediate Cr(VI)-polluted earth and environmental materials.

4. APPLICATIONS

More than a decade after the introduction of SR infrared into the scientific community, SR-FTIR spectromicroscopy applications to research are many. However, most applications have been the characterization of thin sections of fixed or imbedded dry biological samples. In the following section we refer to two studies that demonstrate applications of SR-FTIR to characterize microbial activities that detoxify environmental pollutants in geologic materials in real time. Readers who are interested in other applications are directed to read applications in other related biological, biogeochemical and environmental areas (Benning et al., 2002, 2004a,b; Bonetta et al., 2002; Bradley et al., 2005; Dokken et al., 2005a,b,c; Facciotti et al., 2001; Foriel et al., 2004; Ghosh et al., 2001; Jamme et al., 2008; Jilkine et al., 2008; Kaminskyj et al., 2008; Vogel et al., 2002, 2004; Yee and Benning, 2002; Yee et al., 2003, 2004a,b; Yu et al., 2003, 2004, 2005a,b, 2008). Although we focus on the experimental procedure aspect of the applications, we also demonstrate that a key advantage of the real-time monitoring of microbial activity on the same location of a sample is that the temporal changes in infrared absorption peaks can be quantitative. The latter is especially important since the sample surface can differ and that the absolute value of the absorbance between different samples can vary.

All studies described were performed at Beamline 1.4.3 of the Advanced Light Source at Lawrence Berkeley National Laboratory, Berkeley, CA, using a NicoletMagna760 FTIR bench and Nic-Plan IR microscope in conjunction with a microscope stage environmental chamber (Fig. 4.4). The synchrotron infrared light was focused to a diffraction-limited spot size of 3-10 μm diameter on a computer-controlled *x-y-z* sample stage, and the beam was fiducially located within the field of the microscope to approximately 1 μm, using a titanium pattern on a silicon calibration target. All SR-FTIR measurements were obtained in the reflectance mode in the 4000-650 cm^{-1} region, as this mid-infrared region contains unique molecular absorption fingerprints for the key

molecules of interests in these studies. For each SR-FTIR measurement, 128 spectra were co-added at a spectral resolution of 4 cm^{-1} and their ratio to the spectrum of a bare gold-coated slide was calculated to produce absorbance values. Any residual water vapor features in the resulting spectrum were removed by subtracting an appropriately scaled reference spectrum of water vapor.

The earliest SR-FTIR application to contaminated sediments and minerals was to characterize microbial processes that could detoxify Cr compounds, probably the most widespread toxic and potentially carcinogenic metal pollutant (Holman et al., 1999). It is important to understand the speciation of chromium in a microbe-sediment system because the hazard depends on the chemical state of chromium in those compounds in which Cr occurs. Chromium at its hexavalent state (Cr(VI)) is usually highly soluble in the environment, and therefore the contamination spreads; it is toxic and carcinogenic. Chromium at its pentavalent state (Cr(V)) is usually considered to be more toxic than Cr(VI) because it is more mobile and more reactive with macromolecules in biological systems. However, the relative insolubility of chromium at its trivalent state (Cr(III)) in water renders it significantly less harmful in the environment.

In this real-time SR-FTIR study of microbial reduction of Cr(VI), both the model microbe/mineral and intrinsic microbe/mineral experimental systems were used (Holman et al., 1999). The geologic materials involved were basalt cores that were collected ascetically from 75 meters below the ground surface at a site within the extensive Columbia basalt flow in southeastern Idaho, USA (Fig. 4.5). The site was polluted with mixture of heavy metals and organic vapors including toluene and trichloroethene. The cores were transported aseptically from the site and opened inside a sterile laminar hood to avoid contamination of samples.

For the model microbe/mineral experimental system, it was designed to measure Cr(VI) reduction in the presence of toluene by Cr (VI)-tolerant *Arthrobacter oxydans* on freshly cleaved model mineral magnetite. *A. oxydans* was isolated from the basalt cores (Fig. 4.5), while the magnetite samples were obtained commercially from Minerals Unlimited (Ridgecrest, CA). Magnetite was selected because our earlier investigation revealed a close correlation between the distribution of microbes and of iron oxide-bearing minerals in basalt. The cleaved magnetite chips were cleaned by sonication in deionized and organic-free water and sterilized by ultraviolet irradiation. A 10 μL portion of *A. oxydans* suspension (with cell density of 3×10^8 cells/mL) was introduced onto the magnetite surfaces, and the solvent water was allowed to evaporate slightly (cells remain hydrated) between introductions. The experiment began with a serial introduction of five 10 μL aliquots of 10 μg/L (as chromium) chromate solution onto surfaces of individual magnetite specimens. Five introductions were needed to produce sufficient infrared signals (at the location of observation) throughout the experimental study. Again, solvent water was allowed to evaporate between individual introductions. Localized high concentrations of chromium were observed, because of the heterogeneous surface morphology. All magnetite specimens were incubated in an aerobic atmosphere with 100% relative humidity and diluted toluene vapor inside a 250 mL gas-tight I-CHEM Septa Jars (Fisher Scientific, USA) at room temperature (21 ± 1°C) in the dark. Real-time SR-FTIR spectra for the magnetite experimental system were recorded shortly after the start of the experiment and at the same location, 5 days after the exposure. Spatial distributions of vibrational frequencies associated with intrinsic microorganisms, chromate, toluene, and possible transformed chromium compounds were also mapped after the 5 day exposure. Distinct and relevant infrared

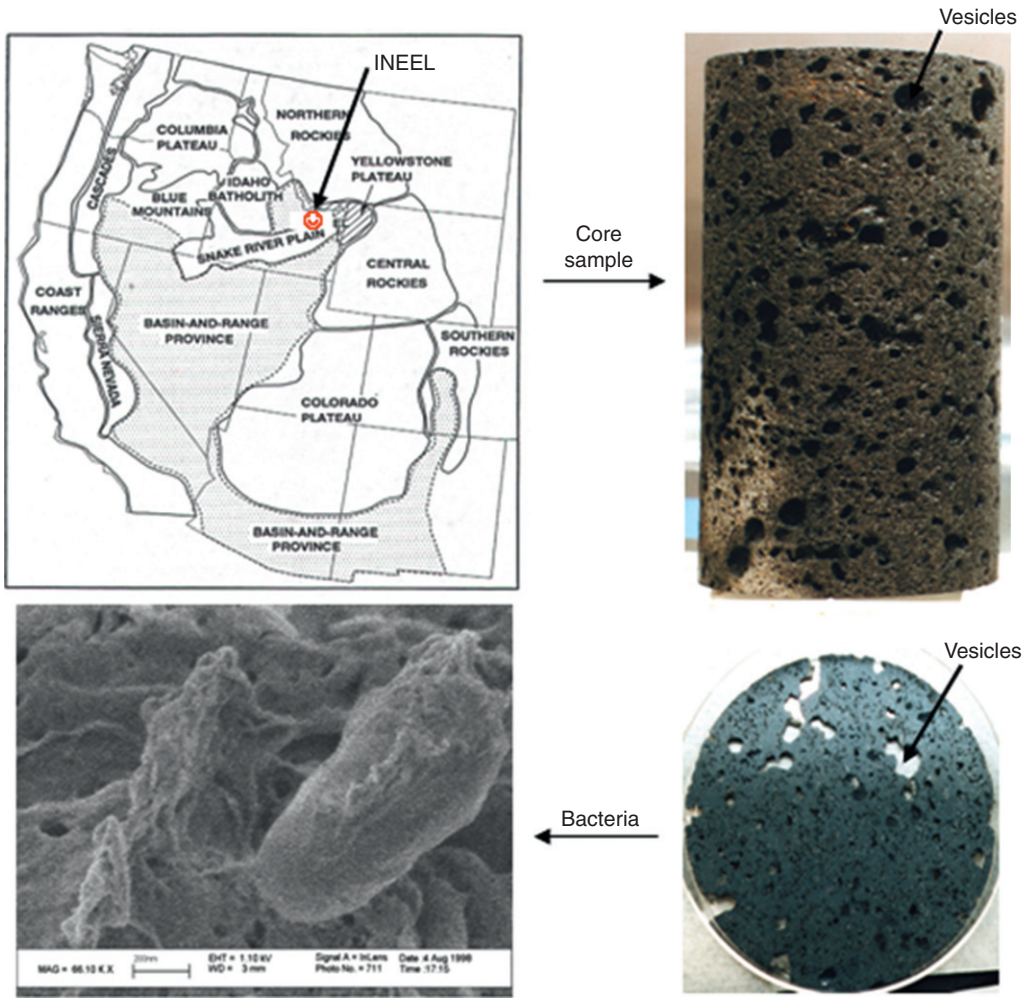

FIGURE 4.5 (Upper left) Map showing regional hydrogeological provinces. The study area, formed from sequences of basalt flows, is within the Eastern Snake River Plain. Sampling location is inside U.S. Department of Energy's Idaho National Engineering and Environmental Laboratory (INEEL). (Upper right) 8.6 cm diameter basalt core samples were collected from 75 m below the ground surface but above the rock aquifer. The sample is fine grained and covered with empty, gas-bubble cavities called vesicles. (Lower right) Section slice of core. (Lower left) SEM image of one of many bacteria types from the core sample.

absorption bands, as summarized in Table 4.3, were used as chemical markers to detect the presence of microorganisms and to identify different chromium species (Fig. 4.6). For magnetite surfaces of mixed iron oxides that contain no living microorganisms, a 5 day exposure to Cr(VI) compounds resulted in statistically insignificant changes in the infrared chemical markers (Fig. 4.6), indicating that little catalysis of Cr(VI) reduction was occurring. On samples with living microorganisms, however, some Cr (VI) reduction was detected. Moreover, when the samples with living microorganisms were incubated in dilute toluene vapor, statistically

TABLE 4.3 Spectral regions and distinct absorption bands within each region for microorganisms (including bacteria), Cr(VI)-, Cr(V)-, and Cr(III)-compounds, toluene, and catechols in our mineral/microorganisms/Cr/toluene system (Holman et al., 1999)

Compounds	Spectral regions (cm^{-1})	Absorption bands (cm^{-1})
Microorganisms (protein)	1800-1500	~1650; ~1550
Cr(VI)-compounds	900-800	~846; ~890
Cr(V)-compounds	900-700	~830; ~764
Cr(III)-compounds	850-750	~810; ~798
Toluene	800-650	~728; ~695
Catechols	800-700	~770; ~742

significant changes in both infrared absorption intensity and characteristic band shapes were observed for Cr(VI), as were new bands signaling the existence of intermediate Cr(V). FTIR spectromicroscopy showed that the changes in the infrared absorption bands occurred at the sites of bacterial concentration. Measured images of the surface at characteristic absorption bands showed a strong correlation between peak depletion of Cr(VI) and depletion of toluene and peak concentration of biological molecules (Fig. 4.7).

For the intrinsic microbe/basalt system, Cr(VI) reduction was monitored on freshly cleaved from the same basalt cores mentioned earlier. Specimens tens of micrometers thick were prepared inside the hood by cleaving basalt fragments off the microfissile near the center of the rock samples. The center of the rock sample was assumed to be unlikely to suffer any

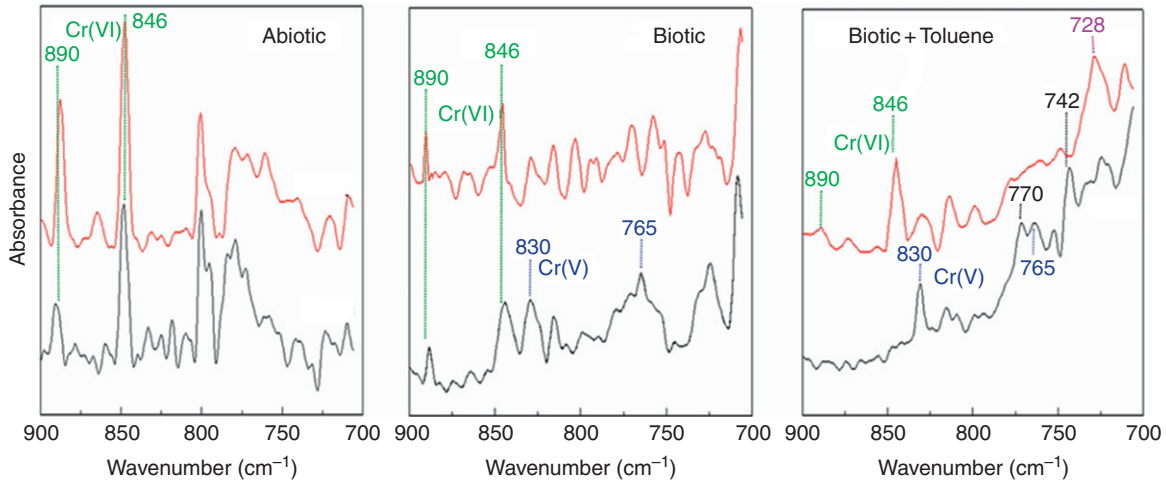

FIGURE 4.6 SR-FTIR spectra of chromate on magnetite surfaces during the 5 day experiment of (left) abiotic reduction, (middle) biotic reduction in the absence of other organic compounds, and (right) biotic reduction in the presence of toluene vapor (as a model volatile organic compound). (—) $t < 1$ day, shifted vertically for visual clarity. (—) $t = 5$ days. Although the total chromate concentration for each of the three experiments were the same, microbial-mineral surface roughness and redistribution during evaporation results in heterogeneous spatial distributions of Cr(VI) concentrations. The most relevant vibrational frequencies identified are marked: 890 and 846 cm^{-1} correspond to Cr(VI), 830 and 765 cm^{-1} correspond to Cr(V), 770 and 742 are catechols, and 728 is toluene. We observe that microbial reduction of Cr(VI) is the dominant mechanism in our experimental system. The microbial chromium reduction is further enhanced during the microbial degradation of the organic compound toluene (Holman et al., 1999).

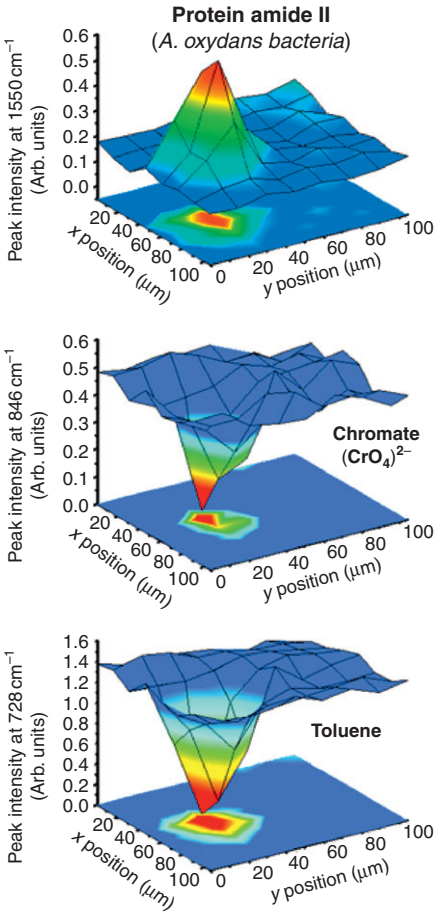

FIGURE 4.7 During the 5 day study period, *Arthrobacter oxydans* bacteria (isolated from the basalt core sample) attached themselves to magnetite surfaces. They reduced Cr(VI) while degrading toluene. SR-FTIR spectromicroscopy measurements at the end of the experiment show the spatial distribution of (top) *A. oxydans*, (middle) chromate, and (bottom) toluene, as measured by their spectral signatures (Holman et al., 1999).

ex situ bacterial contamination from the sample collection and handling processes. The experiment was conducted for four months. The experiment began with the sequential injection of 10 μL of chromate solution onto mineral surfaces in a basalt sample. To minimize the shock of chromate on intrinsic microorganisms, the chromate solution concentration in the injection fluid was gradually increased over a 4 day period: 10, 20, 30, and finally 50 μg/L (as chromium). Individual basalt samples were incubated in the same aerobic atmosphere with 100% relative humidity inside 250 mL gas-tight Septa Jars at room temperature (21 ± 1°C) in the dark. The concentration of toluene vapor was maintained between 80 and 100 μL/L throughout the experiment. A custom IR microscope stage mini-incubator was used to maintain a 100% relative humidity and a constant temperature for microbes while allowing in situ SR-FTIR measurements. Spatial distributions of vibrational frequencies associated with intrinsic microorganisms, chromate, and possibly reduced chromium compounds were mapped at the end of the second week and the end of the fourth month. Results again show that the temporal evolution and spatial distribution of the spectral signatures of chromium of different valence states correlated directly with the distribution of intrinsic microorganisms. Two weeks after the chromate exposure, spectral mappings of microbe-occupied areas of Columbia basalt specimens revealed vibrational frequencies associated with the possible intermediate Cr(V) compounds but not with the possible Cr(III) compounds. In addition, the same spectral mapping reveals a widespread distribution of Cr(V) but an insignificant spatial relationship between the IR absorbance of the possible intermediate Cr(V) compounds and the microbes. The multiple variable analyses shows a small spatial correlation coefficient ($r^2 < 0.01$). A one-way ANOVA, which was used to account for the effect of composite minerals on the spatial relationship between the Cr(VI) reduction to Cr(V) and the distribution of microorganisms, was not significant ($p > 0.1$). At the end of the fourth month, spatial distributions of the same vibrational frequencies 1550 and 830 cm^{-1} are shown in Fig. 4.8. The overall spatial distribution demonstrated an improved correlation between the Cr(VI)

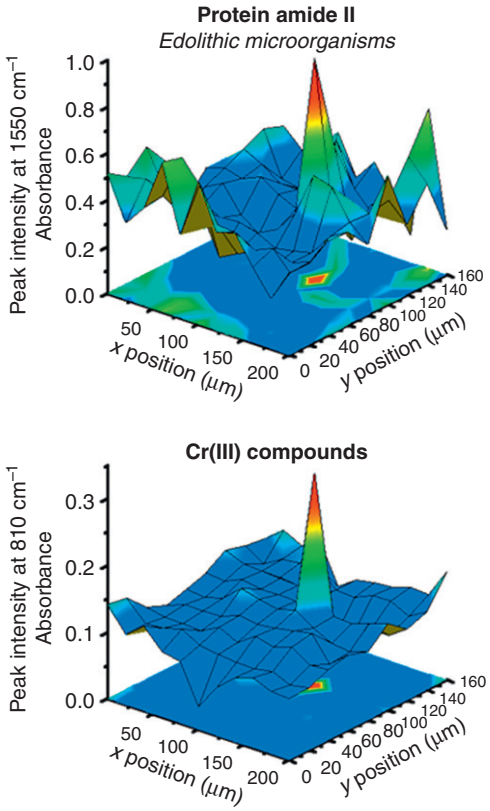

FIGURE 4.8 Distribution of indigenous endolithic microorganisms (top) and the Cr(III) compounds (bottom) as measured by SR-FTIR spectromicroscopy at the end of the 4 month Cr(VI)-microbe-basalt experiment. Only chromium-tolerant and chromium-reducing microorganisms proliferated during the study period (Holman et al., 1999).

reduction to Cr(III) and the distribution of microbes. The lack of vibrational frequencies associated with the presence of possible Cr(III) compounds across the sample surfaces implies that a 2 week duration is only long enough to reduce chromate to its possible intermediate Cr(V) compounds. It is not long enough to reduce Cr(VI) to the final Cr(III) state. Although the multiple variable analysis still shows an insignificant spatial correlation coefficient ($r^2 < 0.01$) for the two measured values, the one-way ANOVA is significant ($p < 0.03$). This implies that a 4 month incubation time has selectively enriched successful growth of chromate-tolerant and -reducing native microbes. The reduced Cr(III) state at the end of the SR-FTIR study was confirmed by X-ray absorption fine structure (XAFS) spectroscopy (Fig. 4.9).

SR-FTIR spectromicroscopy also has been used to examine if humic acid affects microbial destruction of a most recalcitrant toxic organic family of chemicals known as polycyclic aromatic hydrocarbons (PAHs) (Holman et al., 2002). PAHs include more than 100 different chemicals produced by incomplete burning of coal, oil and gas, garbage, tobacco, etc.; many PAHs are carcinogenic. Converting PAHs into nontoxic chemicals removes the hazard, but learning how to do this in an efficient and cost-effective way remains to be accomplished in environmental science.

The role of humic acid (HA) in the biodegradation of toxic polycyclic aromatic hydrocarbons (PAHs) has been controversial. In this study, we used a model system approach to address the controversy. Pyrene was a model PAH, Elliott Soil Humic Acid (ESHA) was the model HA, and *Mycobacterium* sp. JLS (Fig. 4.10) isolated from PAH-contaminated sediments (at the Libby Groundwater Superfund Site in Libby, Montana, USA) was the model microorganism. The mineral substrate was freshly cleaved magnetite also available commercially. Although magnetite is a minor component at the PAH-contaminated site, it efficiently adsorbs both PAHs and bacteria. The basic steps of the procedure employed for the model *Mycobacterium* sp. JLS/magnetite system are illustrated in Fig. 4.11. The magnetite chips were cleaned by sonication in deionized and organic-free water and sterilized by ultraviolet irradiation. Experiment started with the introduction of *Mycobacterium* sp. JLS onto the substrates.

Figure 4.12 summarizes the time series of infrared spectra obtained by repeatedly measuring the same location on each pyrene-coated

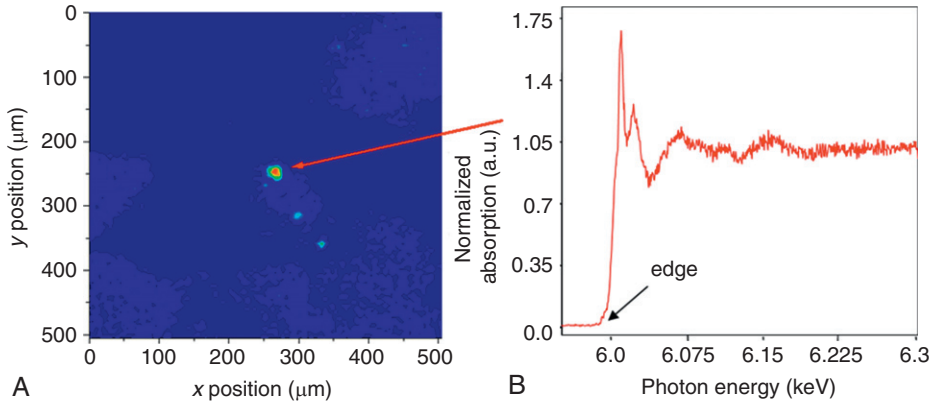

FIGURE 4.9 Confirmation of chromium (III) oxidation state by micro-X-ray analysis on the similar area of the identical sample studied by SR FTIR (see Fig. 4.5). (A) Chromium elemental mapping by micro-X-ray fluorescence analysis (μXRF). The colors go from black (chromium concentration below detection limit) to red (high chromium concentration). (B) Average of 9 micro-X-ray absorption fine structure (μXAFS) scans taken at the highest concentration spot shows no Cr(VI) pre-edge peak and is consistent with Cr(III) compounds. Each data point represents 20 s counting time. The energy increments are 0.5 eV (Holman et al., 1999). Beamline 10.3.2 at the Advanced Light Source at the Lawrence Berkeley National Laboratory was used to collect the μXRF and μXAFS spectrum.

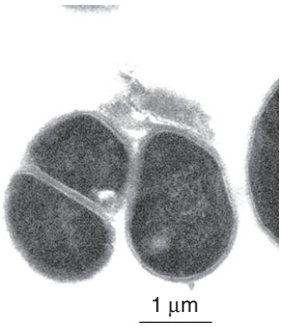

FIGURE 4.10 A TEM image of the newly isolated Gram-positive cocci *Mycobacterium sp.* JLS (GenBank accession no. AF387804). It appears that *M. sp. JLS* degrades polycyclic aromatic hydrocarbons such as pyrene via a novel pathway and gains biomass rapidly while degrading the compounds (Holman et al., 2002). Time-resolved analysis of spectra from SR-FTIR spectromicroscopy did not reveal fingerprints of known metabolites. This is further confirmed by follow-up mass spectrometry analysis of the sample. [Figure courtesy of W.R. Sims].

sample for more than 1 month. Panels a and b (in Fig. 4.12) show details of the IR spectra centered on the pyrene C–H stretching doublet at 3044 and 3027 cm^{-1}, plus peaks from the biomass methyl groups at 2921 and 2850 cm^{-1}. Spectra in panel (a) are for the ESHA-free system, whereas those in panel (b) are for the experimental system containing ESHA. Both panels show that the intensities of the pyrene peaks decrease systematically over time, which corresponds to a reduction in the amount of pyrene present at the measurement location. At the same time, the intensities of the biomass peaks increase, implicating the possibility of microbial utilization of pyrene as a carbon source for growth. By comparing the insets for each panel, it is clear that abiotic processes have little effect. By comparing the trend of the pyrene intensity in these two panels, it appears that ESHA dramatically shortens the onset time for PAH biodegradation from 168 to 2 h (Fig. 4.12). As summarized in Fig. 4.13, in the absence of ESHA, it took the bacteria about 168 h to produce sufficient glycolipids

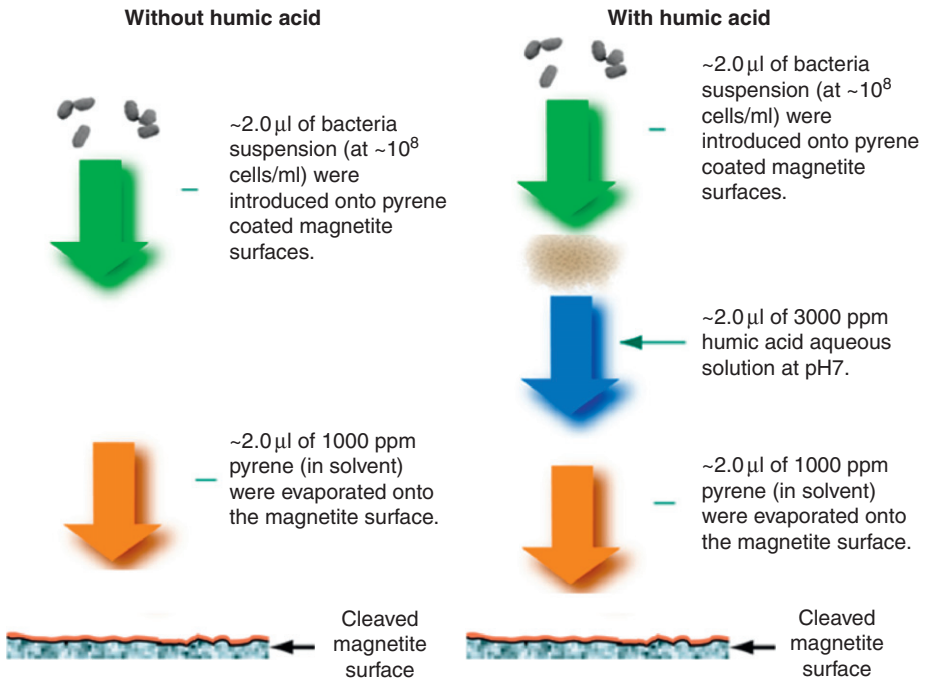

FIGURE 4.11 Basic steps of the model experimental system preparation for the experimental investigation of microbial transformation of pyrene. The magnetite is first cleaned to remove any loose particles and most potential contaminants.

(Holman et al., 2002) to solubilize pyrene. At this point, biodegradation could proceed, resulting in a rapid decrease of pyrene and a rapid increase of biomass within the next 35 h. In the presence of ESHA, pyrene biodegradation began within an hour, and the pyrene was depleted by the end of the fourth hour, with a concurrent increase of biomass (Fig. 4.13). At the end of the time-resolved experiment (about 460 h), spatial distributions of pyrene, *M. sp.* JLS, and ESHA were measured by acquiring infrared spectra at 5 µm intervals across the center of the bacterial colony with HA. Figure 4.14 shows contour maps of the spatial distribution of measured infrared absorbance corresponding to *M. sp.* JLS, HA, and pyrene. The central region of the maps has a high population density of *M. sp.* JLS and a high concentration of HA, but the pyrene in this region was completely biodegraded. Where pyrene is present without *M. sp.* JLS, there is no significant degradation.

5. LIMITATIONS

SR-FTIR spectromicroscopy has intrinsic limitations. The greatest is that not all geologic materials are amenable to infrared measurements (Hofmeister, 1995; Hofmeister et al., 2003). The existence of an infrared reflection-absorption or transmission-absorption spectrum requires that the interaction of mineral crystal or molecules with incident infrared light yields a change in the charge distribution within molecules. Incoming infrared light will be absorbed by the molecule if the following two criteria are met: the frequency of the

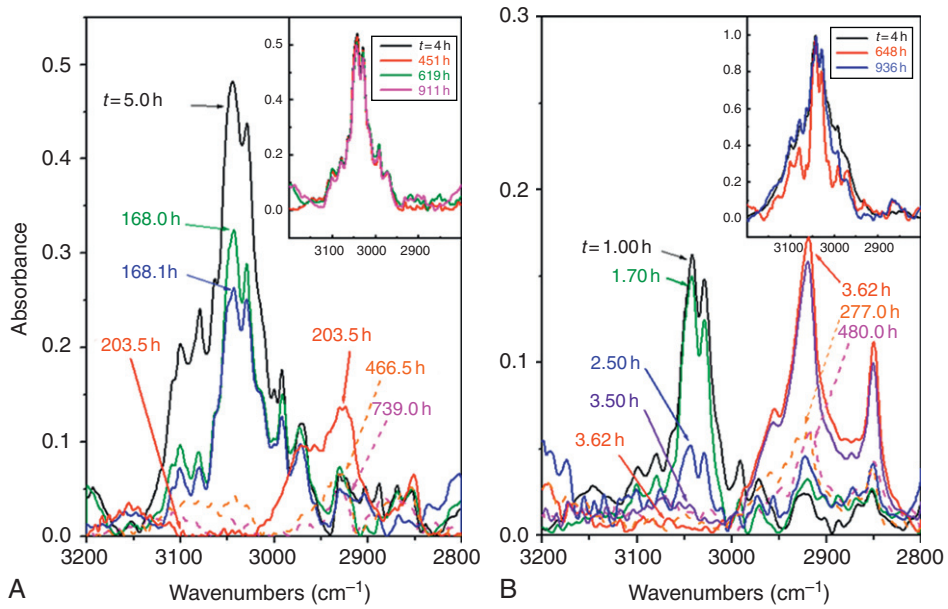

FIGURE 4.12 Time series of SR-FTIR absorption bands corresponding to pyrene and biomass formation following the degradation of pyrene by *Mycobacterium sp*. JLS on magnetite surfaces. Panels a and b are from a sample free of and with ESHA. The time at which each spectrum acquired is labeled. They show the transient behavior of pyrene doublet at 3044 and 3027 cm^{-1} as well as and biomass IR absorption bands at 2921 and 2850 cm^{-1}. Similar behavior was observed for pyrene absorption band centered at 1185 cm^{-1}. Inserts are time series from abiotic control experiments, which show little changes (Holman et al., 2002).

infrared light matches exactly the frequency of a vibrational mode, and the vibration causes an asymmetric change in the charge distribution within the molecule (dipole moment). Almost all earth and environmental materials have vibration frequencies in the mid-infrared region. However, not all earth or environmental materials give rise to a vibration spectrum because the interaction does not cause a change in the dipole moment. For example, many important minerals in soils and sediments science are iron oxides or sulfides, which are often opaque at infrared (as well as visible) wavelengths. Because of this intrinsic limitation, relatively few infrared studies have been on oxides, sulfides, and a several classes of nonsilica bearing minerals. On the other hand, one can more easily monitor microbes and their products with SR-FTIR if the substrate yields no IR spectra.

The ability of SR-FTIR to produce a chemical image with high spatial resolution is limited by the spot size of a SR infrared beam. This spot size has been determined experimentally as $0.73 \times \lambda$, where λ is the wavelength of the infrared light (Levenson et al., 2008a,b). Hence, spatial resolution is generally limited to several micrometers. This limitation can potentially be minimized through near-field spectroscopy (Ikemoto et al., 2008) and imaging compression (Gallet et al., 2008).

Another limitation is that SR-FTIR spectromicroscopy is a time-consuming imaging technique because it uses a single-element infrared

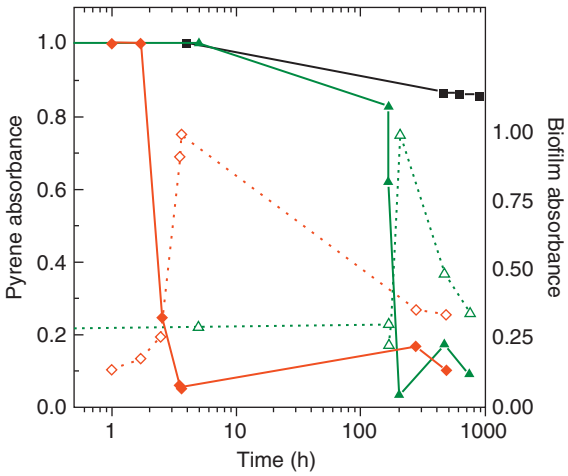

FIGURE 4.13 Summary of the SR-FTIR results showing that pyrene degradation occurs much faster when ESHA is present (note the log scale on the time axis). They pyrene absorbance was measured at 1185 cm^{-1} and biomass IR absorption band at 2921 cm^{-1}. The color scheme is black for abiotic, green for biotic without ESHA, and red for biotic with ESHA. The solid lines show the pyrene amount as a function of time for each experiment. The dotted lines show a subsequent increase in *Mycobacterium* sp. JLS biomass after pyrene degradation (Holman et al., 2002).

detector. A raster-scanned image of a 500 μm-diameter biogeochemical system may take more than an hour to collect. This limitation could be eliminated by using a focal plan array detector. Presently, at least two groups are making progress in this area: the Hirschmugl Group at the University of Wisconsin-Milwaukee and Synchrotron Radiation Center, and the Carr Group at the National Synchrotron Light Source at Brookhaven National Laboratory.

Finally, an unavoidable challenge with using SR-FTIR spectromicroscopy arises from artifacts induced by the mismatch between the refractive index of minerals in sediments and the refractive index adopted by the microscope (Hofmeister, 1995). They shift both peak position and spectral shape. A specimen-specific spectral mini-library helps to detect and correct for these artifacts. That sediments are often heterogeneous with respect to refractive index adds further complexity.

6. PROSPECTS AND CONCLUSIONS

SR-FTIR spectromicroscopy has shown great promise for monitoring microbial activity in soils and sediments as these processes are underway in laboratory environments. This opinion is based on its spatial and temporal resolution, noninvasive measurements, and the simultaneous multiple-component analyses afforded by spectral signatures. As discussed above, synchrotron infrared has significant advantages over conventional infrared spectroscopy in sensitivity and applicability to geologic materials.

Despite that promise, application of SR-FTIR spectromicroscopy to microbial activity in geologic materials has been limited. Synchrotron infrared instruments are not themselves the obstacle. Instead, in the obstacle stems from in the difficulty of rapidly controlling the optimum conditions for an experiment before the products of microbial functions are measured and in optimizing near term data processing and interpretation. Existing techniques are time consuming and labor intensive. Their fragility frequently results in major losses of sample and experimental time, and the many steps required mean it can take days to achieve optimum experimental conditions. An improvement can expand the existing genome-based understanding of microbial activities which would strongly benefit environmental remediation and soils and sediments management science.

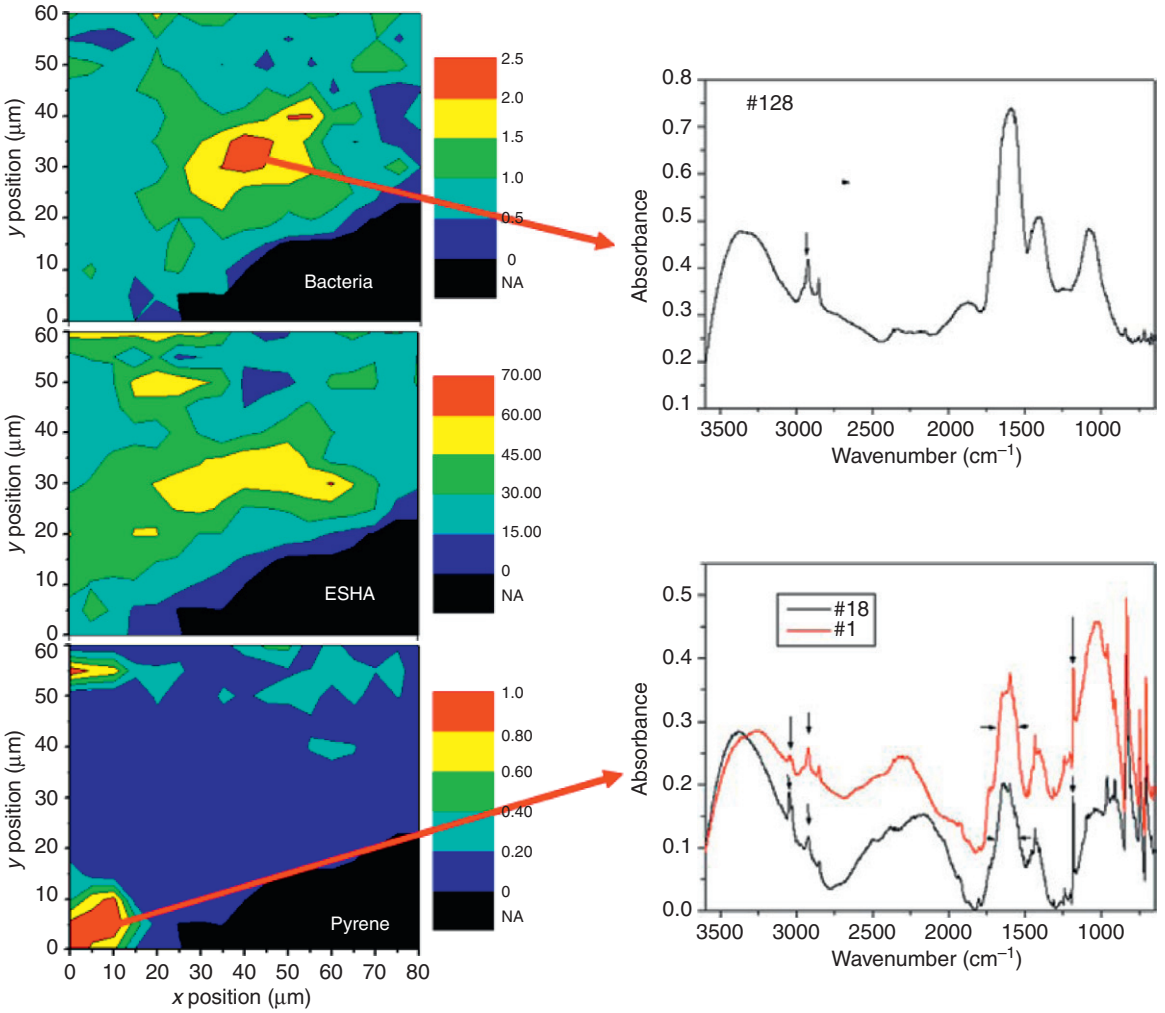

FIGURE 4.14 Contour diagrams from infrared mapping obtained at the end of the experiment showing the spatial distribution of the infrared absorption peaks corresponding to (top) *Mycobacterium sp.* JLS bacteria, (middle) ESHA, and (bottom) pyrene. Appropriate spectral regions were integrated for each point on the maps. The color scales for each contour plot are red for high integrated IR peak area (high concentration of the corresponding component) and blue for low peak area (low concentration); black is an out-of-focus region of the sample. The center of the map shows a region with high density of bacteria and high concentration of ESHA where pyrene has been completely degraded (Holman et al., 2002). Note that the quality of the spectra is excellent even on a complicated surface of geologic materials. (Arrows are pointing at some of marker peaks employed in this study).

ACKNOWLEDGMENTS

This work was performed with support by the Directors of the Office of Science, Office of Biological and Environmental Research, Medical Science Division, the Office of National Petroleum Technology Program, the Office of Science, Basic Energy Sciences, Materials Science Division, of the United States Department of Energy under Contract No. DE-AC03-76SF00098, and the Army Corps of Engineers of the U.S. Department of Defense.

References

Abdullah, H.H., Kubba, R.M., Shanshal, M., 2003. Vibration frequencies shifts of naphthalene and anthracene as caused by different molecular charges. Z. Naturforsch. A J. Phys. Sci. 58, 645–655.

Abuladze, M.K., Asatiani, N.V., Bakradze, N.G., Kartvelishvili, T.M., Holman, H.Y.N., Kalabegishvili, T.L., et al., 2002. Effect of chromium action on the protein composition of Arthrobacter oxydans. Fresenius Environ. Bull. 11, 562–567.

Ahmed-Omer, B., Brandt, J.C., Wirth, T., 2007. Advanced organic synthesis using microreactor technology. Org. Biomol. Chem. 5, 733–740.

Arnold, G., Wagner, C., 1988. Grain-size influence on the mid-infrared spectra of the minerals. Earth Moon Planets 41, 163–171.

Asatiani, N.V., Abuladze, M.K., Kartvelishvili, T.M., Bakradze, N.G., Sapojnikova, N.A., Tsibakhashvili, N.Y., et al., 2004. Effect of chromium(VI) action on arthrobacter oxydans. Curr. Microbiol. 49, 321–326.

Baker, B.J., Moser, D.P., MacGregor, B.J., Fishbain, S., Wagner, M., Fry, N.K., et al., 2003. Related assemblages of sulphate-reducing bacteria associated with ultradeep gold mines of South Africa and deep basalt aquifers of Washington State. Environ. Microbiol. 5, 267–277.

Bantignies, J.L., Moulin, C.C.D., Dexpert, H., Flank, A.M., Williams, G., 1995. Asphaltene adsorption on kaolinite: characterization by infrared microspectroscopy and X-ray-absorption spectroscopy. C. R. Acad. Sci. Ser. Ii 320, 699–706.

Barer, R., 1949. The reflecting microscope in anatomical research. J. Anat. 83, 73–74.

Barer, R., 1953. Determination of dry mass, thickness, solid and water concentration in living cells. Nature 172, 1097–1098.

Barer, G.R., 1954. Quantitative measurements on spreading phenomena in skin. Br. J. Pharmacol. Chemother. 9, 346–351.

Barer, R., Joseph, S., 1954. Refractometry of living cells. 1: basic principles. Q. J. Microsc. Sci. 95, 399–423.

Barer, R., Cole, A.R.H., Thompson, H.W., 1949. Infra-red spectroscopy with the reflecting microscope in physics, chemistry and biology. Nature 163, 198–201.

Bartlett, R.J., James, B.R., Mobility and bioavailability of chromium in soils. In: Nriagu, J.O., Nieboer, E. (Eds.), Chromium in the Natural and Human Environments. Wiley, New York, 1988, pp. 267–304.

Bauschlicher, C.W., 1998. Infrared spectra of polycyclic aromatic hydrocarbons: nitrogen substitution. Chem. Phys. 234, 87–94.

Bauschlicher, C.W., Langhoff, S.R., 1998. Infrared spectra of polycyclic aromatic hydrocarbons: methyl substitution and loss of H. Chem. Phys. 234, 79–86.

Benning, L.G., Yee, N., Phoenix, V., Konhauser, K.O., 2002. The in situ molecular characterisation of a biomineralization process: a synchrotron infrared study. Geochim. Cosmochim. Acta 68, 729–741.

Benning, L.G., Phoenix, V.R., Yee, N., Konhauser, K.O., 2004a. The dynamics of cyanobacterial silicification: an infrared micro-spectroscopic investigation. Geochim. Cosmochim. Acta 68, 743–757.

Benning, L.G., Phoenix, V.R., Yee, N., Tobin, M.J., 2004b. Molecular characterization of cyanobacterial silicification using synchrotron infrared micro-spectroscopy. Geochim. Cosmochim. Acta 68, 729–741.

Beran, A., Langer, K., Andrut, M., 1993. Single-crystal infrared-spectra in the range of Oh fundamentals of paragenetic garnet, omphacite and kyanite in an eklogitic mantle xenolith. Mineral. Pet. 48, 257–268.

Bernstein, M.P., Mattioda, A.L., Sandford, S.A., Hudgins, D.M., 2005. Laboratory infrared spectra of polycyclic aromatic nitrogen heterocycles: quinoline and phenanthridine in solid argon and H_2O. Astrophys. J. 626, 909–918.

Bird, G.R., Blout, E.R., 1952. Infrared microspectroscopy of biologic materials. Lab. Invest. 1, 266–272.

Blout, E.R., 1953. Infrared microspectroscopy: instrumentation and some biological applications. Trans. N Y Acad. Sci. 15, 280–281.

Blout, E.R., Bird, G.R., Grey, D.S., 1950. Infrared microspectroscopy. J. Opt. Soc. Am. 40, 304–312.

Bonetta, D.T., Facette, M., Raab, T.K., Somerville, C.R., 2002. Genetic dissection of plant cell-wall biosynthesis. Biochem. Soc. Trans. 30, 298–301.

Bradley, J., Dai, Z.R., Erni, R., Browning, N., Graham, G., Weber, P., et al., 2005. An astronomical 2175 angstrom feature in interplanetary dust particles. Science 307, 244–247.

Bryant, F.O., Hale, D.D., Rogers, J.E., 1991. Regiospecific dechlorination of pentachlorophenol by dichlorophenol-adapted microorganisms in fresh-water, anaerobic sediment slurries. Appl. Environ. Microbiol. 57, 2293–2301.

Carr, G.L., 1999. High-resolution microspectroscopy and sub-nanosecond time-resolved spectroscopy with the synchrotron infrared source. Vib. Spectrosc. 19, 53–60.

Carrasco-Flores, E.A., Clavijo, R.E., Campos-Vallette, M.M., Aroca, R.F., 2004. Vibrational spectra and surface-enhanced vibrational spectra of 1-nitropyrene. Appl. Spectrosc. 58, 555–561.

Carrasco-Flores, E.A., Clavijo, R.E., Campos-Vallette, M.M., Aroca, R.F., 2005. Vibrational and surface-enhanced vibrational spectra of 6-nitrochrysene. Spectrochim. Acta A Mol. Biomol. Spectrosc. 61, 509–514.

Chauhan, H.P.S., Shaik, N.M., Kori, K., 2004. Synthesis and characterization of some toluene-3,4-dithiolatobismuth (III) alkyl dithiocarbonates. Synth. React. Inorg. Met. Org. Chem. 34, 323–333.

Chinthamreddy, S., Reddy, K.R., 1999. Oxidation and mobility of trivalent chromium in manganese-enriched clays during electrokinetic remediation. J. Soil Contamin. 8, 197–216.

Codd, R., Lay, P.A., 1999. Competition between 1,2-diol and 2-hydroxy acid coordination in Cr(V)-quinic acid complexes: implications for stabilization of Cr(V) intermediates of relevance to Cr(VI)-induced carcinogenesis. J. Am. Chem. Soc. 121, 7864–7876.

Codd, R., Lay, P.A., 2001. Chromium(V)-sialic (neuraminic) acid species are formed from mixtures of chromium(VI) and saliva. J. Am. Chem. Soc. 123, 11799–11800.

Codd, R., Lay, P.A., Levina, A., 1997. Stability and ligand exchange reactions of chromium(IV) carboxylato complexes in aqueous solutions. Inorg. Chem. 36, 5440–5448.

Collins, A.H., 1991. Thermal infrared-spectra and images of altered volcanic-rocks in the Virginia range, Nevada. Int. J. Remote Sens. 12, 1559–1574.

da Silva, M., Cerniglia, C.E., Pothuluri, J.V., Canhos, V.P., Esposito, E., 2003. Screening filamentous fungi isolated from estuarine sediments for the ability to oxidize polycyclic aromatic hydrocarbons. World J. Microbiol. Biotechnol. 19, 399–405.

Delineau, T., Allard, T., Muller, J.P., Barres, O., Yvon, J., Cases, J.M., 1994. Ftir reflectance vs Epr studies of structural iron in kaolinites. Clays Clay Miner. 42, 308–320.

Dillon, C.T., Lay, P.A., Cholewa, M., Legge, G.J.F., Bonin, A.M., Collins, T.J., et al., 1997. Microprobe X-ray absorption spectroscopic determination of the oxidation state of intracellular chromium following exposure of V79 Chinese hamster lung cells to genotoxic chromium complexes. Chem. Res. Toxicol. 10, 533–535.

Dinsdale, E.A., Edwards, R.A., Hall, D., Angly, F., Breitbart, M., Brulc, J.M., et al., 2008. Functional metagenomic profiling of nine biomes. Nature 452, 629–632.

Dokken, K.M., Davis, L.C., Erickson, L.E., Castro-Diaz, S., Marinkovic, N.S., 2005a. Synchrotron fourier transform infrared micro spectroscopy: a new tool to monitor the fate of organic contaminants in plants. Microchem. J. 81, 86–91.

Dokken, K.M., Davis, L.C., Marinkovic, N.S., 2005b. Use of infrared microspectroscopy in plant growth and development. Appl. Spectrosc. Rev. 40, 301–326.

Dokken, K.M., Davis, L.C., Marinkovic, N.S., 2005c. Using SR-IMS to study the fate and transport of organic contaminants in plants. Spectroscopy 20, 14.

Ehrlich, H.L., 1994. Special issue: breakthroughs in karst geomicrobiology and redox geochemistry—foreword. Geomicrobiol. J. 12, 135.

Ehrlich, H.L., 1998. Geomicrobiology: its significance for geology. Earth Sci. Rev. 45, 45–60.

Ehrlich, H.L., 2000. Geomicrobiology. Geotimes 45, 34–37.

Eyring, E.M., Wadsworth, M.E., 1956. Differential infrared spectra of adsorbed monolayers-normal-hexanethiol on Zn minerals. Trans. Am. Inst. Min. Metall. Eng. 205, 531–535.

Facciotti, M.T., Rouhani, S., Burkard, F.T., Betancourt, F.M., Downing, K.H., Rose, R.B., et al., 2001. Structure of an early intermediate in the M-state phase of the bacteriorhodopsin photocycle. Biophys. J. 81, 3442–3455.

Farmer, V.C. (Ed.), 1974. The Infrared Spectra of Minerals. Mineralogical Society, London.

Foriel, J., Philippot, P., Susini, J., Dumas, P., Somogyi, A., Salome, M., et al., 2004. High-resolution imaging of sulfur oxidation states, trace elements, and organic molecules distribution in individual microfossils and contemporary microbial filaments. Geochim. Cosmochim. Acta 68, 1561–1569.

Furukawa, K., 2000. Biochemical and genetic bases of microbial degradation of polychlorinated biphenyls (PCBs). J. Gen. Appl. Microbiol. 46, 283–296.

Furukawa, K., 2003. 'Super bugs' for bioremediation. Trends Biotechnol. 21, 187–190.

Furukawa, K., Hirose, J., Suyama, A., Zaiki, T., Hayashida, S., 1993. Gene components responsible for discrete substrate-specificity in the metabolism of biphenyl (Bph operon) and toluene (Tod operon). J. Bacteriol. 175, 5224–5232.

Furukawa, K., Suenaga, H., Goto, M., 2004. Biphenyl dioxygenases: functional versatilities and directed evolution. J. Bacteriol. 186, 5189–5196.

Gallet, J., Riley, M., Hao, Z., Martin, M.C., 2008. Increasing FTIR spectromicroscopy speed and resolution through compressive imaging. Infrared Phys. Technol. 51, 420–422.

Gez, S., Luxenhofer, R., Levina, A., Codd, R., Lay, P.A., 2005. Chromium(V) complexes of hydroxamic acids: formation, structures, and reactivities. Inorg. Chem. 44, 2934–2943.

Ghosh, U., Talley, J.W., Luthy, R.G., 2001. Particle-scale investigation of PAH desorption kinetics and thermodynamics from sediment. Environ. Sci. Technol. 35, 3468–3475.

Gore, R.C., 1949. Infrared spectrometry of small samples with the reflecting microscope. Science 110, 710–711.

Griffith, W.P., Lewis, J., Wilkinson, G., 1959. Infrared spectra of transition metal-nitric oxide complexes. 4. The pentacyanonitrosyl-complexes of chromium and molybdenum. J. Chem. Soc. 872–875.

Guilhaumou, N., Dumas, P., Carr, G.L., Williams, G.P., 1998. Synchrotron infrared microspectrometry applied to petrography in micrometer-scale range: fluid chemical analysis and mapping. Appl. Spectrosc. 52, 1029–1034.

Ha, Y.W., Stack, R.J., Hespell, R.B., Gordon, S.H., Bothast, R.J., 1991. Some chemical and physical-properties of extracellular polysaccharides produced by butyrivibrio-fibrisolvens strains. Appl. Environ. Microbiol. 57, 2016–2020.

Hale, D.D., Rogers, J.E., Wiegel, J., 1990. Reductive dechlorination of dichlorophenols by nonadapted and adapted microbial communities in pond sediments. Microb. Ecol. 20, 185–196.

Hale, D.D., Rogers, J.E., Wiegel, J., 1991. Environmental-factors correlated to dichlorophenol dechlorination in anoxic fresh-water sediments. Environ. Toxicol. Chem. 10, 1255–1265.

Hawkins, N.J., Mattraw, H.C., Sabol, W.W., Carpenter, D.R., 1955. Spectroscopy of gaseous carbonyls. 1. Infrared spectra and thermodynamic properties of chromium and molybdenum hexacarbonyls. J. Chem. Phys. 23, 2422–2427.

Hines, M.E., Orem, W.H., Lyons, W.B., Jones, G.E., 1982. Microbial activity and bioturbation induced oscillations in pore water chemistry of estuarine sediments in spring. Nature 299, 433–435.

Hofmeister, A.M., 1995. Infrared microspectroscopy in earth science. In: Brame, E.G. (Ed.), Practical Guide to Infrared Microspectroscopy. Marcel Dekker, Inc., New York, pp. 377–416.

Hofmeister, A.M., Keppel, E., Speck, A.K., 2003. Absorption and reflection infrared spectra of MgO and other diatomic compounds. Mon. Not. R. Astron. Soc. 345, 16–38.

Holman, H.Y.N., Perry, D.L., Martin, M.C., Lamble, G.M., McKinney, W.R., Hunter-Cevera, J.C., 1999. Real-time characterization of biogeochemical reduction of Cr(VI) on basalt surfaces by SR-FTIR imaging. Geomicrobiol. J. 16, 307–324.

Holman, H.Y.N., Nieman, K., Sorensen, D.L., Miller, C.D., Martin, M.C., Borch, T., et al., 2002. Catalysis of PAH biodegradation by humic acid shown in synchrotron infrared studies. Environ. Sci. Technol. 36, 1276–1280.

Holman, H.Y.N., Martin, M.C., McKinney, W.R., 2003. Synchrotron-based FTIR spectromicroscopy: cytotoxicity and heating considerations. J. Biol. Phys. 29, 275–286.

Holman, H.Y.N., Miles, R., Hao, Z., Wozei, E., Anderson, L.M., Yang, H., 2009a. Real-time chemical imaging of bacterial activity in biofilms using open-channel microfluidics and synchrotron ftir spectromicroscopy. Anal. Chem. 81, 8564–8570.

Holman, H.Y.N., Wozei, E., Lin, Z., Comolli, L.R., Ball, D.A., Borglin, S., et al., 2009b. Real-time molecular monitoring of chemical environment in obligate anaerobes during oxygen adaptive response. Proc. Natl. Acad. Sci. USA 106, 12599–12604.

Hudgins, D.M., Bauschlicher, C.W., Allamandola, L.J., Fetzer, J.C., 2000. Infrared spectroscopy of matrix-isolated polycyclic aromatic hydrocarbon ions. 5. PAHs incorporating a cyclopentadienyl ring. J. Phys. Chem. A 104, 3655–3669.

Hudgins, D.M., Sandford, S.A., 1998a. Infrared spectroscopy of matrix isolated polycyclic aromatic hydrocarbons. 1. PAHs containing two to four rings. J. Phys. Chem. A 102, 329–343.

Hudgins, D.M., Sandford, S.A., 1998b. Infrared spectroscopy of matrix isolated polycyclic aromatic hydrocarbons. 2. PAHs containing five or more rings. J. Phys. Chem. A 102, 344–352.

Hudgins, D.M., Sandford, S.A., 1998c. Infrared spectroscopy of matrix isolated polycyclic aromatic hydrocarbons. 3. Fluoranthene and the benzofluoranthenes. J. Phys. Chem. A 102, 353–360.

Humphrey, R.E., 1961. The infrared spectra of aromatic chromium tricarbonyls. Spectrochim. Acta 17, 93–100.

Ikemoto, Y., Moriwaki, T., Okamura, H., Sasaki, T., Yoneyama, N., Taguchi, A., et al., 2008. Broad band infrared near-field spectroscopy at finger print region using SPring-8. Infrared Phys. Technol. 51, 417–419.

International Agency for Research on Cancer, IARC, 1990. Monographs on the evaluation of the carcinogenic risk of chemicals to humans. International Agency for Research on Cancer, Lyon, France.

Jamme, F., Robert, P., Bouchet, B., Saulnier, L., Dumas, P., Guillon, F., 2008. Aleurone cell walls of wheat grain: high spatial resolution investigation using synchrotron infrared microspectroscopy. Appl. Spectrosc. 62, 895–900.

Janni, J., Gilbert, B.D., Field, R.W., Steinfeld, J.I., 1997. Infrared absorption of explosive molecule vapors. Spectrochim. Acta A Mol. Biomol. Spectrosc. 53, 1375–1381.

Jensen, J.O., 2004. Vibrational frequencies and structural determination of phosphorus tricyanide. Spectrochim. Acta A Mol. Biomol. Spectrosc. 60, 2537–2540.

Jensen, J.O., Jensen, J.L., 2004. Vibrational frequencies and structural determination of trimethylarsine oxide. Spectrochim. Acta A Mol. Biomol. Spectrosc. 60, 3065–3070.

Jilkine, K., Gough, K.M., Julian, R., Kaminskyj, S.G.W., 2008. A sensitive method for examining whole-cell biochemical composition in single cells of filamentous fungi using synchrotron FTIR spectromicroscopy. J. Inorg. Biochem. 102, 540–546.

Kalabegishvili, T.L., Tsibakhashvili, N.Y., Holman, H.Y.N., 2003. Electron spin resonance study of chromium(V) formation and decomposition by basalt-inhabiting bacteria. Environ. Sci. Technol. 37, 4678–4684.

Kaminskyj, S., Jilkine, K., Szeghalmi, A., Gough, K., 2008. High spatial resolution analysis of fungal cell biochemistry: bridging the analytical gap using synchrotron FTIR spectromicroscopy. FEMS Microbiol. Lett. 284, 1–8.

Kashefi, K., Holmes, D.E., Reysenbach, A.L., Lovley, D.R., 2002. Use of Fe(III) as an electron acceptor to recover previously uncultured hyperthermophiles: isolation and characterization of *Geothermobacterium ferrireducens* gen. nov., sp nov. Appl. Environ. Microbiol. 68, 1735–1742.

Keller, W.D., Spotts, J.H., Biggs, D.L., 1952. Infrared spectra of some rock-forming minerals. Am. J. Sci. 250, 453–471.

Kim, Y.H., Pak, K., Pothuluri, J.V., Cerniglia, C.E., 2004. Mineralization of erythromycin A in aquaculture sediments. FEMS Microbiol. Lett. 234, 169–175.

Kretzschmar, R., Robarge, W.P., Weed, S.B., 1993. Flocculation of kaolinitic soil clays: effects of humic substances and iron-oxides. Soil Sci. Soc. Am. J. 57, 1277–1283.

Kumamaru, T., Suenaga, H., Mitsuoka, M., Watanabe, T., Furukawa, K., 1998. Enhanced degradation of polychlorinated biphenyls by directed evolution of biphenyl dioxygenase. Nat. Biotechnol. 16, 663–666.

Levenson, E., Lerch, P., Martin, M.C., 2006. Infrared imaging: synchrotrons vs. arrays, resolution vs. speed. Infrared Phys. Technol. 49, 45–52.

Levenson, E., Lerch, P., Martin, M.C., 2008a. Spatial resolution limits for synchrotron-based infrared spectromicroscopy. Infrared Phys. Technol. 51, 413–416.

Levenson, E., Lerch, P., Martin, M.C., 2008b. Spatial resolution limits for synchrotron-based spectromicroscopy in the mid- and near-infrared. J. Synchrotron Radiat. 15, 323–328.

Levina, A., Barr-David, G., Codd, R., Lay, P.A., Dixon, N.E., Hammershoi, A., et al., 1999. In vitro plasmid DNA cleavage by chromium(V) and -(IV) 2-hydroxycarboxylato complexes. Chem. Res. Toxicol. 12, 371–381.

Levina, A., Codd, R., Dillon, C.T., Lay, P.A., 2003. Chromium in biology: toxicology and nutritional aspects. Prog. Inorg. Chem. (51), 145–250.

Levina, A., Codd, R., Foran, G.J., Hambley, T.W., Maschmeyer, T., Masters, A.F., et al., 2004. X-ray absorption spectroscopic studies of chromium(V/IV/III)2-ethyl-2-hydroxybutanoato(2-/1-) complexes. Inorg. Chem. 43, 1046–1055.

Li, J.F., Fuller, S., Cattle, J., Way, C.P., Hibbert, D.B., 2004. Matching fluorescence spectra of oil spills with spectra from suspect sources. Anal. Chim. Acta 514, 51–56.

Lijour, Y., Gentric, E., Deslandes, E., Guezennec, J., 1994. Estimation of the sulfate content of hydrothermal vent bacterial polysaccharides by Fourier-transform infrared-spectroscopy. Anal. Biochem. 220, 244–248.

Lu, R., Goncharov, A., Mao, H.K., Hemley, R., 1999. Synchrotron infrared microspectroscopy: applications to hydrous minerals. In: Schulze, D.G., Stucki, J.W., Bertsch, P.M. (Eds.), Synchrotron X-Ray Methods in Clay Sciences. The Clay Mineral Society, Boulder, Colorado, pp. 164–182.

Ludwig, C., Dolny, M., Gotze, H.J., 2000. Fourier transform Raman and infrared spectra and normal coordinate analysis of organo-arsenic(III), -antimony(III) and -bismuth(III) thiolates. Spectrochim. Acta A Mol. Biomol. Spectrosc. 56, 547–555.

Luys, M.J., Deroy, G., Vansant, E.F., Adams, F., 1982. Characteristics of asbestos minerals: structural aspects and infrared-spectra. J. Chem. Soc. Faraday Trans. I 78, 3561–3571.

Lyons, W.B., Gaudette, H.E., Armstrong, P.B., 1979. Evidence for organically associated iron in nearshore pore fluids. Nature 282, 202–203.

Macalady, J., Banfield, J.F., 2003. Molecular geomicrobiology: genes and geochemical cycling. Earth Planet. Sci. Lett. 209, 1–17.

Mattioda, A.L., Hudgins, D.M., Bauschlicher, C., Allamandola, L.J., 2002. Infrared spectra of matrix-isolated polycyclic aromatic hydrocarbons and their ions: PAHs incorporating the peropyrene structure. Abstr. Pap. Am. Chem. Soc. 224, U323.

McKinney, W.R., Martin, M.C., Chin, M., Portman, G., Melczer, M.E., Watson, J.A., 2000. 4 Axis Implementation of the Active Feedback Mirror System for the IR Beamline 1.4.3. ALS Compendium.

Mielczarski, J.A., Cases, J.M., Bouquet, E., Barres, O., Delon, J.F., 1993. Nature and structure of adsorption layer on apatite contacted with oleate solution. 1. Adsorption and Fourier-transform infrared reflection studies. Langmuir 9, 2370–2382.

Misawa, N., Shindo, K., Takahashi, H., Suenaga, H., Iguchi, K., Okazaki, H., et al., 2002. Hydroxylation of various molecules including heterocyclic aromatics using recombinant Escherichia coli cells expressing modified biphenyl dioxygenase genes. Tetrahedron 58, 9605–9612.

Mou, X.Z., Sun, S.L., Edwards, R.A., Hodson, R.E., Moran, M.A., 2008. Bacterial carbon processing by generalist species in the coastal ocean. Nature 451, 708–711.

Newman, D.K., Banfield, J.F., 2002. Geomicrobiotogy: how molecular-scale interactions underpin biogeochemical systems. Science 296, 1071–1077.

Nguyen, T.T., Janik, L.J., Raupach, M., 1991. Diffuse reflectance infrared Fourier-transform (drift) spectroscopy in soil studies. Aust. J. Soil Res. 29, 49–67.

Nriagu, J.O., Historical perspectives. In: Nriagu, J.O., Nieboer, E. (Eds.), Chromium in the Natural and Human Environments. Wiley-Interscience, New York, 1988, pp. 1–19.

Panero, W.R., Benedetti, L.R., Jeanloz, R., 2003. Transport of water into the lower mantle: role of stishovite. J. Geophys. Res. Solid Earth 108, 355–366.

Pauzat, F., Ellinger, Y., 2001. The 3.2-3.5 μm region revisited—II. A theoretical study of the effects of hydrogenation on some model PAHs. Mon. Not. R. Astron. Soc. 324, 355–366.

Pauzat, F., Ellinger, Y., 2002. The infrared signatures of non-regular PAHs. Chem. Phys. 280, 267–282.

Plesko, E.P., Scheetz, B.E., White, W.B., 1992. Infrared vibrational characterization and synthesis of a family of hydrous alkali uranyl silicates and hydrous uranyl silicate minerals. Am. Mineral. 77, 431–437.

Pothuluri, J.V., Selby, A., Evans, F.E., Freeman, J.P., Cerniglia, C.E., 1995. Transformation of chrysene and other polycyclic aromatic hydrocarbon mixtures by the fungus cunninghamella-elegans. Can. J. Bot. 73, S1025–S1033.

Pothuluri, J.V., Doerge, D.R., Churchwell, M.I., Fu, P.P., Cerniglia, C.E., 1998a. Fungal metabolism of nitrofluoranthenes. J. Toxicol. Environ. Health A 53, 153–174.

Pothuluri, J.V., Sutherland, J.B., Freeman, J.P., Cerniglia, C.E., 1998b. Fungal biotransformation of 6-nitrochrysene. Appl. Environ. Microbiol. 64, 3106–3109.

Pothuluri, J.V., Freeman, J.P., Fu, P.P., Cerniglia, C.E., 1999. Biotransformation of 1-nitrobenzo[e]pyrene by the fungus Cunninghamella elegans. J. Ind. Microbiol. Biotechnol. 22, 52–57.

Povarennykh, A.S., 1978. Use of infrared-spectra for determination of minerals. Am. Mineral. 63, 956–959.

Revsbech, N.P., Sorensen, J., Blackburn, T.H., Lomholt, J.P., 1980. Distribution of oxygen in marine-sediments measured with microelectrodes. Limnol. Oceanogr. 25, 403–411.

Reysenbach, A.L., Shock, E., 2002. Merging genomes with geochemistry in hydrothermal ecosystems. Science 296, 1077–1082.

Rossman, G.R., Aines, R.D., 1991. The hydrous components in garnets—Grossular—Hydrogrossular. Am. Mineral. 76, 1153–1164.

Ruiterkamp, R., Halasinski, T., Salama, F., Foing, B.H., Allamandola, L.J., Schmidt, W., et al., 2002. Spectroscopy of large PAHs: laboratory studies and comparison to the diffuse interstellar bands. Astron. Astrophys. 390, 1153–1170.

Salmassi, T.M., Venkateswaren, K., Satomi, M., Nealson, K.H., Newman, D.K., Hering, J.G., 2002. Oxidation of arsenite by Agrobacterium albertimagni, AOL15, sp nov., isolated from Hot Creek, California. Geomicrobiol. J. 19, 53–66.

Scarvie, T., Andresen, N., Baptiste, K., Byrd, J., Chin, M., Martin, M.C., et al., 2004. Noise reduction efforts for the ALS infrared beamlines. Infrared Phys. Technol. 45, 403–408.

Seelenbinder, J.A., Brown, C.W., 2002. Comparison of organic self-assembled monolayers as modified substrates for surface-enhanced infrared absorption spectroscopy. Appl. Spectrosc. 56, 295–299.

Sham, T.K., Rivers, M.L., 2002. A brief overview of synchrotron radiation. Appl. Synchrotron Radiat. Low Temp. Geochem. Environ. Sci. 49, 117–147.

Snow, E.T., 1991. A Possible role for chromium(Iii) in genotoxicity. Environ. Health Perspect. 92, 75–81.

Solomon, D., Lehmann, J., Kinyangi, J., Liang, B.Q., Schafer, T., 2005. Carbon K-edge NEXAFS and FTIR-ATR spectroscopic investigation of organic carbon speciation in soils. Soil Sci. Soc. Am. J. 69, 107–119.

Sorensen, J., Jorgensen, B.B., Revsbech, N.P., 1979. Comparison of oxygen, nitrate, and sulfate respiration in coastal marine-sediments. Microb. Ecol. 5, 105–115.

Sreedhara, A., Susa, N., Rao, C.P., 1997. Vanadate and chromate reduction by saccharides and L-ascorbic acid: effect of the isolated V(IV) and Cr(III) products on DNA nicking, lipid peroxidation, cytotoxicity and on enzymatic and non-enzymatic antioxidants. Inorg. Chim. Acta 263, 189–194.

Stern, R.M., 1982. Biological and environmental aspects of chromium. In: Langard, S. (Ed.), Biological and Environmental Aspects of Chromium. Elsevier, Amsterdam.

Suenaga, H., Mitsuoka, M., Ura, Y., Watanabe, T., Furukawa, K., 2001. Directed evolution of biphenyl dioxygenase: emergence of enhanced degradation capacity for benzene, toluene, and alkylbenzenes. J. Bacteriol. 183, 5441–5444.

Suenaga, H., Watanabe, T., Sato, M., Ngadiman, K., Furukawa, 2002. Alteration of regiospecificity in biphenyl dioxygenase by active-site engineering. J. Bacteriol. 184, 3682–3688.

Teetsov, S.A., 1995. Unique preparation techniques for nanogram samples. In: Brame, E.G. (Ed.), Practical Guide to Infrared Microspectroscopy. Marcel Dekker, Inc., New York, pp. 417–443.

Todd, M.W., Provencal, R.A., Owano, T.G., Paldus, B.A., Kachanov, A., Vodopyanov, K.L., et al., 2002. Application of mid-infrared cavity-ringdown ectroscopy to trace explosives vapor detection using a broadly tunable (6-8 mu m) optical parametric oscillator. Appl. Phys. B Lasers Opt. 75, 367–376.

Tsibakhashvili, N.Y., Asatiani, N.V., Abuladze, M.K., Birkaya, B.G., Sapojnikova, N.A., Mosulishvili, L.M., et al., 2002a. Capillary electrophoresis of Cr(VI) reducer Arthrobacter oxydans. Biomed. Chromatogr. 16, 327–331.

Tsibakhashvili, N.Y., Mosulishvili, L.M., Kalabegishvili, T.L., Pataraya, D.T., Gurielidze, M.A., Nadareishvili, G.S., et al., 2002b. Chromate-resistant and reducing-microorganisms in georgia basalts: their distribution and characterization. Fresenius Environ. Bull. 11, 352–361.

Tsibakhashvili, N.Y., Mosulishvili, L.M., Kalabegishvili, T. L., Kirkesali, E.I., Frontasyeva, M.V., Pomyakushina, E. V., et al., 2004. ENAA studies of chromium uptake by Arthrobacter oxydans. J. Radioanal. Nucl. Chem. 259, 527–531.

Tsou, T.C., Lin, R.J., Yang, J.L., 1997. Mutational spectrum induced by chromium(III) in shuttle vectors replicated in human cells: relationship to Cr(III)-DNA interactions. Chem. Res. Toxicol. 10, 962–970.

Vilas, F., Jarvis, K.S., Gaffey, M.J., 1994. Iron alteration minerals in the visible and near-infrared spectra of low-albedo asteroids. Icarus 109, 274–283.

Vogel, J.P., Raab, T.K., Schiff, C., Somerville, S.C., 2002. PMR6, a pectate lyase-like gene required for powdery mildew susceptibility in Arabidopsis. Plant Cell 14, 2095–2106.

Vogel, J.P., Raab, T.K., Somerville, C.R., Somerville, S.C., 2004. Mutations in PMR5 result in powdery mildew resistance and altered cell wall composition. Plant J. 40, 968–978.

Voitkun, V., Zhitkovich, A., Costa, M., 1998. Cr(III)-mediated crosslinks of glutathione or amino acids to the DNA phosphate backbone are mutagenic in human cells. Nuclic Acids Res. 26, 2024–2030.

Wetzel, D.L., LeVine, S.M., 1999. Microspectroscopy: imaging molecular chemistry with infrared microscopy. Science 285, 1224–1225.

White, J.L., 1971. Interpretation of infrared spectra of soil minerals. Soil Sci. 112, 22.

Yee, N., Benning, L.G., 2002. In situ FTIR study of protonation reactions at the bacteria-water interface. Geochim. Cosmochim. Acta 66, A862.

Yee, N., Phoenix, V.R., Konhauser, K.O., Benning, L.G., Ferris, F.G., 2003. The effect of cyanobacteria on silica precipitation at neutral pH: implications for bacterial silicification in geothermal hot springs. Chem. Geol. 199, 83–90.

Yee, N., Benning, L.G., Konhauser, K.O., 2004a. Silica colloid aggregation by cyanobacteria: a microbial silicification mechanism. Geochim. Cosmochim. Acta 68, A199.

Yee, N., Benning, L.G., Phoenix, V.R., Ferris, F.G., 2004b. Characterization of metal-cyanobacteria sorption reactions: a combined macroscopic and infrared spectroscopic investigation. Environ. Sci. Technol. 38, 775–782.

Yu, P., 2005a. Molecular chemistry imaging to reveal structural features of various plant feed tissues. J. Struct. Biol. 150, 81–89.

Yu, P.Q., 2005b. Application of cluster analysis (CLA) in feed chemical imaging to accurately reveal structural-chemical features of feeds and plants within cellular dimension. J. Agric. Food Chem. 53, 2872–2880.

Yu, P.Q., 2008. Molecular chemistry of plant protein structure at a cellular level by synchrotron-based FTIR spectroscopy: comparison of yellow (Brassica rapa) and Brown (Brassica napus) canola seed tissues. Infrared Phys. Technol. 51, 473–481.

Yu, P.Q., McKinnon, J.J., Christensen, C.R., Christensen, D. A., Marinkovic, N.S., Miller, L.M., 2003. Chemical imaging of microstructures of plant tissues within cellular dimension using synchrotron infrared microspectroscopy. J. Agric. Food Chem. 51, 6062–6067.

Yu, P., Christensen, D.A., Christensen, C.R., Drew, M.D., Rossnagel, B.G., McKinnon, J.J., 2004. Use of synchrotron FTIR microspectroscopy to identify chemical differences in barley endosperm tissue in relation to rumen degradation characteristics. Can. J. Anim. Sci. 84, 523–527.

Zhang, Y., Yang, M., Dou, X.M., He, H., Wang, D.S., 2005. Arsenate adsorption on an Fe-Ce bimetal oxide adsorbent: role of surface properties. Environ. Sci. Technol. 39, 7246–7253.